Lack of gastric acidification reduces postprandial energy expenditure and protein digestion but not growth in *Astyanax mexicanus*

Patrícia Gomes Ferreira[1,*], Hugo Flávio[1,2] and Jonathan M. Wilson[1,*]

[1]Department of Biology, Wilfrid Laurier University, Waterloo, Ontario Canada

[2]Department of Biology, Dalhousie University, Halifax, Nova Scotia, Canada

[*]Correspondent authora
Patrícia Gomes Ferreira
Email: patricia.ferreira@uottawa.ca
Jonathan M. Wilson
Email: jmwilson@wlu.ca

Abstract

The vertebrate stomach is responsible for the secretion of hydrochloric acid (HCl) and is the first site of protein digestion in the gut. The secretion of HCl occurs through the gastric proton pump, a hydrogen-potassium ATPase (HKA) composed of α and β subunits encoded by the *ATP4A* and *ATP4B* genes, respectively. In the past, the evidence for the role of the gastric acid secretion in nutrient digestion and absorption, growth, and postprandial energy metabolism has been gathered using indirect methods such as diet modulation experiments, or the use of proton-pump inhibitors. These methods may introduce confounding factors and lead to erroneous conclusions. With the aim of directly observing the role of the gastric proton pump,

Journal of Experimental Biology • Accepted manuscript

we have generated a knockout (KO) model using targeted gene editing. Using *atp4a*-null *Astyanax mexicanus*, we examined the growth rate, nitrogen and energy metabolism, and nutrient assimilation in the presence and absence of gastric acidification. Our results show no effect of KO on growth or appetite, but a significant reduction in post-prandial nitrogen excretion and oxygen consumption (specific dynamic action). Furthermore, *atp4a*$^{-/-}$ animals had significantly less body magnesium, calcium, phosphorus and protein, while having more lipid in their carcasses. Importantly, administration of proton-pump inhibitors suppressed growth in both experimental groups indicating possible off-target effects of these drugs. This study is the first to directly examine the impact of gastric acidification on body composition, growth and metabolism and offers new and targeted evidence on the importance of stomach acidification for gut and digestion homeostasis.

Introduction

The capacity for acid-peptic digestion was a major innovation in the evolution of the digestive system that gave rise to the stomach phenotype of vertebrates (Koelz, 1992; Smit, 1968). Acid production is essential for the activation of pepsinogen into the aspartic peptidase pepsin; an important enzyme in protein digestion (Kageyama, 2002; Richter et al., 1998). In addition, acid secretion has been shown to be important for the solubilization of phosphorus (P), and consequently calcium (Ca) fixation in bones, as well as magnesium (Mg) absorption (Sugiura, 2025; Kopic and Geibel 2013). Gastric acid secretion is performed by the highly conserved gastric proton pump (HKA), a heterodimeric enzyme encoded by the *ATP4A* gene (α subunit) and the *ATP4B* gene [β subunit; (Shin et al., 2009)]. In spite of the importance and conservation of acid-peptic digestion in vertebrates, secondary loss is not uncommon (Koelz 1992; Castro et al., 2014; Kato et al., 2024; Ferreira et al. 2025a)

The secretion of gastric acid into the stomach lumen during digestion is driven by the ATP-dependent movement of hydrogen ions (H^+) against a large gradient (160 mM) in exchange

for potassium cations [K^+; (Kopic et al., 2010; Shin et al., 2009)]. The intracellular H^+ (and bicarbonate; HCO_3^-) are produced by the hydration of carbon dioxide (CO_2) catalyzed by cytoplasmic carbonic anhydrase in the oxynticopeptic cells of the gastric glands of fish ($CO_2 + H_2O \rightleftharpoons H_2CO_3 \rightleftharpoons H^+ + HCO_3^-$). The apical secretion of H^+ is complemented with the basolateral secretion of HCO_3^- into the blood (Ferreira et al. 2025b). This in turn generates a transient acid-base imbalance called the postprandial alkaline tide (first described by Jones, 1845, and reviewed by Niv and Fraser 2002). The alkaline tide has been widely characterized in mammals (Brunton, 1933; Niv & Fraser, 2002) and more recent studies have characterized it in several fish species, from chondrichthyans (Wood et al., 2007) to teleosts (Bucking et al., 2009; Cooper & Wilson, 2008). In fish, the immediate recovery of acid-base homeostasis is achieved through the excretion of HCO_3^- mainly by the gills before HCO_3^- is secreted into the anterior intestine to neutralize the acidic chyme (reviewed by Wood, 2019). This recovery process presumably contributes to the overall energetic cost associated with the maintenance of the gastric proton pump.

Pharmacological inhibition of acid secretion through the use of omeprazole, a proton pump inhibitor (Shin & Sachs, 2008), has been associated with a reduction in growth in Nile tilapia (*Oreochromis niloticus*) as a probable consequence of reduced protein digestibility (Moffatt et al., 2022). The gastric proton pump is essential for the initiation of protein digestion in the stomach (Kageyama, 2002). The pepsinogens, secreted by the oxynticopeptic cell, are activated in the presence of hydrochloric acid (HCl) and are the first peptidases to act on the chyme. The dietary amino acids that are not used in protein synthesis are not stored in the body, unlike lipids and carbohydrates (Chandel 2021). Thus, after absorption, excess dietary amino acids are catabolized, and fish experience an overall increase in ammonia levels (NH_3 and NH_4^+) in the plasma and consequent increased ammonia excretion into the water through the gills (Bucking et al., 2009; Kaushik & de Oliva Teles, 1985). This increase in ammonia is largely due to the catabolism of digested protein and the metabolism of the gut tissue and liver (Taylor et al., 2010; Rubino et al., 2014). The secretion of gastric acid activates a pH-sensitive response

in the anterior intestine that triggers the release of intestinal hormones such as cholecystokinin (CCK; Holstein 1982; Holmgren and Holmberg 2005; Volkoff et al. 2005). The secreted CCK binds to CCKb receptors in the pyloric sphincter's smooth muscle and in afferent vagal neurons leading to a decrease in stomach motility and, consequently, to a delay in the rate of gastric emptying in mammals (Smith et al. 1984; Lin and Miller 1992; Corp et al. 1993; Olsson et al. 1999). Moffatt et al. (2022) showed significantly increased gastric emptying rates in Nile tilapia after omeprazole treatment, supporting the physiological importance of gastric acid in the regulation of gastric transit time. In addition, gastric bypass surgery has been linked to decreased gastrointestinal transit time in mice (Liou et al., 2013).

The energetic costs associated with nutrient ingestion, digestion, and assimilation are commonly termed specific dynamic action (SDA) and translate into a transient, post prandial elevation of metabolic rate (Chabot et al., 2016). Studies over the past decades have comprehensively examined this phenomenon in various taxa and found that it significantly contributes to an animal's energy budget (Beamis et al., 1975; Fu et al., 2005; Goodrich et al., 2022; Secor, 2009). The SDA response is likely to include a broad set of processes spanning from pre- to post- absorptive phases of digestion. While several studies have attempted to examine the contribution of the gastric acid digestion to the magnitude of SDA using proton pump inhibitors or diet modulation, the results have been contradictory and species dependent (Andrade et al., 2005; Goodrich et al., 2022; Nørgaard et al., 2016; Secor, 2009). Since acid secretion by the gastric proton pump is an ATP dependent process with a stoichiometry of 1 H^+:1 ATP, there will be a direct cost of acid secretion. The estimates of H^+s pumped per O_2 consumed range from 5.0 to 2.3 (Kopic et al. 2010; Bannister 1985, respectively. See Goodrich et al., 2022a). However, it is clear that a significant component of SDA is tied to processes that include increased rates of protein synthesis (37.2 mmol ATP or 6.2 mmol O_2 per gram protein synthesis; Houlihan et al. 1993) and the metabolism of nutrients after intestinal absorption (Brown & Cameron, 1991a, 1991b; Lyndon et al., 1992; Smith & Houlihan, 1995) but a more broad understanding of the contributors to the SDA remains to be fully characterized.

The use of HKA-null animals (which lack gastric acidification) is an excellent tool for clarifying the specific role of gastric acid in growth and to further dissect the components and allocation of postprandial energy utilization, and illuminate the consequence of the evolutionary loss of the stomach phenotype (Ferreira et al. 2025a). In the present study, we compared energy consumption, body composition, nitrogen excretion, acid-base homeostasis, and growth in previously generated knockout (*atp4a*$^{-/-}$) and wild-type (*atp4a*$^{+/+}$) *Astyanax mexicanus* (Ferreira et al. 2025b). The Mexican tetra, *A. mexicanus*, is a small freshwater fish that is emerging as a powerful evo-dev model organism (Swaminathan et al., 2024). The knockout fish are achlorhydric, with circumneutral stomach pH levels, and lower acid-peptic gene (e.g. *atp4b, pga, pgc*) expression in contrast to wild type fish that notably have a post-prandial stomach pH of 3.8 (Ferreira et al. 2025b). We hypothesized that the absence of gastric acidification in *atp4a*$^{-/-}$ fish decreases the magnitude both of the SDA (measured by intermittent flow respirometry) and of the alkaline tide. Furthermore, we predicted that *atp4a*$^{-/-}$ fish would experience impaired protein digestion, reduced growth, and faster gastric transit times. An alternative scenario could reflect that the reduction in the energetic cost of digestion would enhance fish growth and food conversion efficiency. To characterize the impacts of gastric acidification on mineral and protein digestion, we analyzed Mg, Ca, P, total protein, and lipid content in the carcass. Finally, to assess potential secondary targets of the proton pump inhibitor omeprazole, we included a two-week omeprazole treatment in our growth trial.

Materials and Methods

Animals

Astyanax mexicanus (surface morph) were originally obtained from the Tabin lab Harvard Medical School (Boston USA). Fish were maintained as described previously in Ferreira et al., (2025b), and kept at 22.5°C in recirculation systems with artificial freshwater: reverse osmosis

water adjusted to 700-800 µS cm^{-1} with sea salt (Instant Ocean). All animal experiments were approved by the Animal Care Committee at Wilfrid Laurier University (AUP R22002). The knockout line for *atp4a* was previously characterized by (Ferreira et al. 2025b). The mutant animals have a net +16 bp change in exon 11 that results in a premature stop codon 536 aa downstream of the start codon of Atp4a, resulting in a truncated and non-functional protein resulting in the loss of gastric acidification. Henceforth, we refer to wild-type animals as *atp4a*$^{+/+}$, and homozygous knockout animals as *atp4a*$^{-/-}$.

Growth trials

Homozygous (*atp4a*$^{-/-}$) and wild-type (*atp4a*$^{+/+}$) fish (1.5 months old, mixed sex, n = 10) were placed in individual containers in a recirculating aquatic rack system supplied with artificial freshwater kept at 22.5°C. The food was carefully weighed on a precision balance. The weighing of the micro-pellets (feed) was reproducible and a pilot feeding trial was conducted beforehand to ensure feasibility. The fish were habituated to the system and feed [Tropical micro pellets, Hikari. See supplementary information for pellet dietary formulation)] for two weeks prior to starting the trial. Fish were weighed on an analytical balance, after briefly blotting the excess water from their body, (KO 0.0865 ± 0.0342 g; WT 0.1155 ± 0.0486 g) at the beginning of the trial and fed a 3% body mass (BM) daily ration. The fish consumed the entire meal within a few minutes. Recirculation was paused for 15min before feeding until 1h post feed. We ensured that the entire meal was consumed before re-starting the system's recirculation. Ration size was adjusted on a weekly basis following re-weighing. After three weeks of regular diet feed (Control period), all animals were switched to a diet supplemented with omeprazole to evaluate possible off-target effects of this proton-pump inhibitor (omeprazole period). After two weeks on the omeprazole diet, fish were switched back to the regular diet (Hikari, 3% BM) for three weeks (Recovery period). Specific growth rates (SGR = G) were calculated following Crane et al. (2020), as follows:

$$G = 100(e^g - 1), \qquad e^g = (\frac{m_2}{m_1})^{\frac{1}{\Delta t}}$$

Where ***g*** is the instantaneous growth rate, ***e*** is the natural log, m_1 and m_2 represent initial and final mass, respectively, and Δt represents the elapsed time between measurements (days). The feed conversion ratios (FCR) were calculated for each group and trial week by dividing the feed intake (mg) by the mass gain (mg).

Omeprazole diet preparation

Omeprazole (Tokyo Chemical Industry) was added to the Hikari pellets in a dose of 25 mg kg^{-1} day^{-1} dissolved in 95% ethanol based on a 3% BM ration (Wood et al., 2009; Moffatt et al. 2022). In short, the pellets were air dried to completely evaporate the ethanol, stored at -20°C, and used within a week.

Acid-base fluxes

Homozygous and wild-type (WT) animals (n = 8 per group) were fasted for 48h prior to the acid-flux measurements. On the morning of the fluxes, the animals were voluntarily fed a 5% BM bloodworm meal and transferred to aerated static flux chambers (50 mL). The water samples were collected at 0, 3, 6, 9 and 24 h after transfer. The fish were transferred back to their original containers after the 24 h flux period and the faeces were collected from the chambers and dried at 60°C for later total nitrogen quantification. The titratable alkalinity of chamber water samples was measured following McDonald and Wood (1981) by titrating 10 mL of water to an endpoint of pH 4.3 with an autoburette/titrator system (Radiometer Copenhagen ABU 80 autoburette/TTT 80 titrator), followed by a manual titration to an endpoint of pH 4.0 with 0.01 N HCl (Sigma-Aldrich). The total ammonia in the water was measured using the salicylate-based

colourimetric method following Cooper and Wilson (2008) based on Verdouw et al. (1978). The net fluxes of titratable alkalinity (J_{TAlk}) and total ammonia (J_{TAmm}) for each flux period were calculated using the following equation from Cooper and Wilson (2008):

$$J_{netX} = \frac{([X]_i - [X]_f) \times V}{(M \times t)}$$

where $[X]_i$ and $[X]_f$ are the initial and final values for ammonia (µM TAN) or titratable alkalinity (µEq L^{-1}), V is the volume of water (L), M is mass of the fish (kg), and t is the duration of the flux period (h). The difference between J_{TAlk} and J_{TAmm} (µmol kg^{-1} h^{-1}) was used to calculate the net acid-base flux (µEq kg^{-1} h^{-1}). The faeces excreted during the acid flux measurements were collected and dried at 60°C for later determination of the total nitrogen content. Before drying, faeces were photographed using a Leica M165FC stereomicroscope with a DFC6200 camera. The relative length of the faeces was measured in the LASX software, with a minimum of 20 faecal pellets measured per animal (n = 6 animals per genotype).

Respirometry

The oxygen consumption rate ($\dot{M}_{O_2}$ in µmol O_2 g^{-1} h^{-1}) was determined using intermittent flow respirometry. Details on the system setup, phase duration, and methods of $\dot{M}_{O_2}$ and SDA calculation are provided in Supplementary Material.

The day before the experiment, the animals were weighed (to the nearest 0.0001 g using an analytical balance) to determine the ration size. The following day, the animals were voluntarily fed (5% BM wet bloodworm meal) 15-20 min before being placed inside the respirometers. The respirometers were covered with a black plastic tube to minimize visual stimuli. Measurements of $\dot{M}_{O_2}$ were initiated immediately after the transfer of each animal to the respirometer. The animals were allowed to remain in the chambers undisturbed for 24 h (pilot trials showed that this time sufficed to capture SDA and standard metabolic rate; SMR). In total, 26 animals were

used in these experiments, resulting in 20 post-prandial traces deemed appropriate for SDA estimations. Five animals were excluded because they showed high activity levels throughout the experiment, (high noise levels in the measurement points/O_2) preventing an accurate estimation of SDA. One last animal was excluded because it displayed a very short SDA (approx. 3h), so it is likely to have vomited the meal. Of the 20 animals used for the analysis, 8 were *atp4a*$^{+/+}$ (0.40 ± 0.04 g), and 12 were *atp4a*$^{-/-}$ (0.35 ± 0.03 g). The $\dot{M}O_2$ for each cycle was determined using the R package pyroresp (Flávio, 2025), in R v4.4.1 (R Core Team, 2024).

Appetite trial

The appetite levels of KO and WT fish were determined following a modified appetite assay from Aspiras et al. (2015). Animals (n = 8 per group) were fasted for 48 h and then offered a pre-weighed (~0.5 g) bloodworm meal. After 24 h, the remaining bloodworms were separated from fecal matter and reweighed. The appetite results were normalized to the condition factor ($K = 100\ BM\ (g)\ Length\ (cm)^{-3}$; Ricker, 1975; Aspiras et al. 2015).

Tissue sampling

Fish (*atp4a*$^{-/-}$ n = 12, *atp4a*$^{+/+}$ n = 8) were fed a bloodworm meal (5% BM) and euthanized three hours post feeding with an overdose Tricaine Methanesulfonate (1:5000 Syndel, Nanaimo BC) buffered with $NaHCO_3$ to pH 7. The stomach contents were emptied and weighed to determine stomach emptying. In addition to stomach, the brain and intestine (after removal of the chyme) were also snap frozen and kept at -80°C until further use. The remaining organs were excised from the body cavity, and the carcasses weighed, dried at 85°C, and weighed again for total water determination.

Compositional and element carcass analyses

All dried carcasses, feed, and faeces were manually ground using a mortar and pestle into a powder and kept in moisture-free conditions until further analysis. Total lipid content was determined gravimetrically in ground carcasses using established methods (AOAC, 2000, detailed methods can be found in the Supplemental material). The Mg, Ca, Na and P content in the carcasses and feed were quantified through inductively coupled plasma-optical emission spectroscopy (Optima 8000 ICP-OES spectrometer, Perkin Elmer). Twenty mg of dried-ground carcass and feed (pellets and bloodworms) were weighed and transferred to clean glass culture tubes containing 2 mL of 20% (v:v) nitric acid (HNO_3). The tubes were heated at 105°C for 30 min and manually agitated every 10 min. After digestion of the sample, the tubes were cooled to room temperature, and the contents were transferred to a clean 15 mL capped tube with the volume adjusted to 15 mL with ultrapure water. The samples were centrifuged for 5 min (EC Clinical Centrifuge Damon) and transferred to new clean 15 mL tubes. Elemental standards (sodium phosphate monobasic, calcium chloride dihydrate, and magnesium chloride hexahydrate) were prepared in a final concentration of 1000 mg/L, following the same protocol as the preparation of the sample, including digestion in HNO_3.

The total nitrogen content of the dry-ground carcass and faecal samples was determined using a 2400 CHNS analyzer (Perkin Elmer). One to three mg of dry sample was used, and acetanilide (71.09% C, 6.71% H, 10.36% N; BDH Organic Analytical Standard) was used as a standard to verify calibration before and during the analysis. Total nitrogen was converted to protein using the standard conversion coefficient of 6.25 and the final values expressed as a percentage of protein per dry mass (Mariotti et al. 2008).

Determination of ammonia content in the chyme and feed

The quantification of ammonia in the chyme and the feed (bloodworm meal) was carried out using a commercial assay (ammonia assay kit AA0100-1KT, Sigma kit; glutamate dehydrogenase

method). PNH_3 in the chyme was determined using pK' and α NH_3 values reported for 23°C by Cameron and Heisler (1983), and ionic strength was assumed to be 125 mM (Rubino et al., 2014). NH_3 and PNH_3 were calculated following Rubino et al. (2014).

Gene expression

Total RNA from the brain and intestine samples was extracted using a RNeasy Mini Kit with on-column DNase treatment (Qiagen, Hilden, Germany). One µg of total RNA was converted into cDNA using the High-Capacity cDNA RT kit (Applied Biosystems). Quantitative real-time PCR (qPCR) was used to evaluate gene expression profiles of genes related to growth, gastric evacuation, and satiation (Table 1), using the BlasTaq™ 2X qPCR Master Mix (Applied Biological Materials Inc., Richmond BC) on a BioRad CFX96 real time system under the following cycle conditions: denaturation 95°C 3 min, and forty cycles of 95°C for 15 s, 58°C for 30 s and 72°C for 2 s. Melt curve analysis was performed after each run to confirm single band products. Relative expression levels were normalized with a geometric mean using the elongation factor (*ef1a*), *18s* and *gapdh* gene expression. Reference gene primer sequences were previously published by Imarazene (2020) *(ef1a* and *18s*) and Ferreira et al. 2025b (*gapdh*). Relative gene expression quantification was calculated using the $2^{-\Delta\Delta CT}$ method (Livak & Schmittgen, 2001).

Cholecystokinin ELISA

Frozen anterior intestine samples (3 h post prandial) were homogenized in phosphate-buffered saline (PBS) using a bead homogenizer (Precellys 24; 6500 RPM for 2 x 10 s; Bertin) and centrifuged at 21.1k × g for 15 min at 4°C. A fish specific CCK ELISA assay was used to measure expression (Cusabio Tech LLC). The total protein concentration of samples was determined using the BCA assay with a BSA standard. CCK is expressed as pg CCK μg^{-1} protein.

Data analyses

Before we tested for differences between treatment groups, the normality of the data was verified by a Shapiro-Wilk test, followed by a homoscedasticity test. For most datasets, differences between the two groups were tested with a two-tailed independent t-test (when data were normally distributed) or a Wilcoxon rank sum test (when data were not normally distributed). For the analysis of the growth and flux data, a Two-Way Repeated Measures ANOVA was used, followed by a Tukey HSD post hoc test. For the respirometry data, because variance was unequal between the groups for the four variables of interest (i.e. SMR, SDA duration, SDA net peak, and SDA magnitude), differences between the groups were tested using Welsh two sample t-tests. P-values lower than 0.05 were considered statistically significant. All statistical analyses were performed in R 4.4.0. Data are presented as mean ± SEM.

Results

Lack of gastric acid does not impact growth in *A. mexicanus* but illustrates potential off-target effects of omeprazole

The specific growth rates (SGR) were calculated weekly during the eight weeks of the growth trial (Figure 1A). The fish consumed the entire 3% BM meal in less than 3h. The mass of the two groups was not significantly different from each other at the beginning of the trial (*atp4a*$^{+/+}$ 0.0865 ± 0.0342 g, *atp4a*$^{-/-}$ 0.1155 ± 0.0486 g, t_{18} = 1.570, p = 0.134). The SGR were similar between genotypes throughout the 8 weeks (p = 0.670). There was no interaction between genotype and trial period weeks (Control 1-3, Omeprazole 1-2 and Recovery 1-3. F (7, 125) = 0.506, p = 0.829). Both groups had a significantly reduced SGR in the second week of omeprazole treatment (~45.2% reduction). This depression in growth rates was sustained up until the last week of the recovery phase (week 8 of the trial), at which time both groups showed recovery to control levels of growth. Although no differences in SGRs were detected

between genotypes, the final body mass at the end of the trial indicated KO were smaller than WT fish: *atp4a*$^{+/+}$ 0.3234 ± 0.0217 g, *atp4a*$^{-/-}$ 0.2469 ± 0.0313 g, t_{18} = 2.258, p = 0.037. The feed conversion rate (FCR) did not differ between genotypes (p = 0.967) and there was no interaction between genotype and trial period (interaction F (7, 126) = 0.796, p = 0.592; Figure 1B). The FCR was significantly higher compared to the control levels in the second week of omeprazole treatment, returning to levels similar to control from week 7 of the trial period.

Lack of gastric acid reduces branchial ammonia excretion with no discernible impact on acid-base

The ammonia excretion rate (J_{Tamm}) to the water was elevated during the first 24 h post feed in both genotypes and was 3.65 fold higher in *atp4a*$^{+/+}$ compared to *atp4a*$^{-/-}$ fish following feeding and until 24h post-feed (Figure 2A). No significant changes were observed between groups in titratable alkalinity (J_{Talk}, see Supplementary Figure S1). The net acid-base flux was calculated as the difference between J_{Tamm} and J_{TAlk}, with negative values indicative of net base uptake (i.e. acid excretion) and positive values indicative of net base excretion (i.e. acid uptake). The acid-base fluxes showed elevated base uptake levels in *atp4a*$^{+/+}$ animals during the first 24 h and remained unchanged in *atp4a*$^{-/-}$ animals (with net positive values) throughout the same time period. Both groups showed positive flux values (base excretion) at 30h post feed, albeit significantly higher in *atp4a*$^{-/-}$ animals (p-value interaction < 0.01; Figure 2B). The bloodworm meal ammonia content averaged 0.077 ± 0.003 µmol total ammonia nitrogen (TAN). The cumulative amount of ammonia excreted above baseline levels was significantly higher (approximately 5-fold) in *atp4a*$^{+/+}$ in relation to *atp4a*$^{-/-}$ fish (Figure 2C). The percentage of excreted ammonia corresponding to direct absorption (i.e. excluding catabolism) from the meal (%TAN in meal) was calculated by dividing the excreted TAN over the baseline (µmol) by the amount of ammonia in the meal ingested. This value was significantly higher in *atp4a*$^{-/-}$ animals (t_9 = 3.181 p = 0.011, Figure 2D). The total ammonia (Tamm) concentration was measured in

the gastric chyme and was found to be more than 50% higher in *atp4a*$^{-/-}$ fish (2.55 ± 0.31 mM) relative to *atp4a*$^{+/+}$ fish (1.65 ± 0.17 mM, $t_{27} = 2.486$, $p = 0.019$).

Reduced Specific Dynamic action magnitude and duration in *atp4a*$^{-/-}$*A. mexicanus*

The post prandial $\dot{M}_{O_2}$ of *atp4a*$^{+/+}$ and *atp4a*$^{-/-}$ fish is shown in Figure 3A. The two genotypes had a similar SMR (*atp4a*$^{+/+}$: 5.42 ±0.40 µmol O_2 g^{-1} h^{-1} *atp4a*$^{-/-}$: 5.10 ±0.35 µmol O_2 g^{-1} h^{-1}, $t_{15.9}$ = 0.418, p = 0.681), establishing a solid baseline for further comparisons (Figure 3E). The SDA duration of *atp4a*$^{-/-}$ fish was significantly reduced by 11.0% compared to *atp4a*$^{+/+}$ fish (*atp4a*$^{+/+}$ 15.25 ± 0.55 h, *atp4a*$^{-/-}$ 13.58 ± 0.41 h, $t_{14.1} = 2.432$, $p = 0.029$; Figure 3C). The net peak of SDA, on the other hand, was similar between groups (*atp4a*$^{+/+}$ 3.03 ± 0.18 µmol O_2 g^{-1} h^{-1} *atp4a*$^{-/-}$ 2.80 ± 0.12 µmol O_2 g^{-1} h^{-1},$t_{12.6}$ = 1.034, p = 0.321; Figure 3D). Finally, SDA magnitude was significantly reduced by 16.8% in *atp4a*$^{-/-}$ animals relatively to *atp4a*$^{+/+}$ fish (*atp4a*$^{+/+}$ 21.47 ± 1.43 µmol O_2 g^{-1} h^{-1} and *atp4a*$^{-/-}$ 16.78 ± 0.94 µmol O_2 g^{-1} h^{-1}, $t_{12.8} = 2.745$, $p = 0.017$; Figure 3B).

Lack of stomach acidification does not produce significant changes to appetite.

The appetite analysis did not reveal differences between genotypes (Supplemental Table 1). Likewise, no differences were found in the condition factor (Fulton, K) nor in gastric evacuation (Supplemental Table 1). Finally, no differences were found in any of the genes linked to satiation analyzed in the brain tissues (Supplemental Figure S2).

Gastric acid influences carcass mineral composition

The carcass composition analyses revealed significantly lower levels of Mg, Ca, and P, in *atp4a*$^{-/-}$ fish (40%, 53%, 62% reduction, in Mg, Ca and P, respectively, Figure 4A-C). The levels of

sodium (Na) remained unaltered between genotypes (10.0 ± 0.6 mg·g^{-1} of dry carcass *atp4a*$^{+/+}$, 10.0 ± 0.6 mg·g^{-1} of dry carcass *atp4a*$^{-/-}$, Supplemental Figure S3). The *atp4a*$^{+/+}$ group had a significantly higher carcass moisture content than *atp4a*$^{-/-}$ fish (Figure 4D). Total carcass protein levels were significantly decreased in *atp4a*$^{-/-}$ fish (Figure 4E). In contrast, *atp4a*$^{-/-}$ animals had a significantly higher carcass lipid content compared to *atp4a*$^{+/+}$ animals (Figure 4F).

Gastric acid knockout decreases digestibility and exarcebates protein fecal loss

The faeces of the two groups differed greatly in appearance, with *atp4a*$^{-/-}$ faeces showing more intact bloodworms (Figure 5E,F) compared to visually more digested faeces excreted by *atp4a*$^{+/+}$ animals (Figure 5A,B). The length of the digested bloodworms was used as a proxy for the degree of digestion. The overall length of individual faeces was greater in *atp4a*$^{-/-}$ fish (Figure 5C). The percentage of protein in the fecal matter was also more than 2-fold higher in *atp4a*$^{-/-}$ animals (Figure 5D).

Cholecystokinin levels are negatively impacted by lack of gastric acid

At 3 h post feeding, the CCK mRNA levels in anterior intestine were significantly lower in *atp4a*$^{-/-}$ fish (t_{12} = 2.562, p = 0.024; Figure 6A). The CCK peptide concentration in the anterior intestine of *atp4a*$^{+/+}$ fish was 60% lower in *atp4a*$^{-/-}$ fish as well (t_7 = 2.456, p = 0.044, Figure 6B).

Discussion

The inhibition of the gastric proton pump acid secretion through targeted gene knockout (*atp4a*$^{-/-}$) had profound effects on postprandial energy utilization and protein, lipid and mineral

(P, Mg, Ca) balance but did not affect growth in juvenile *A. mexicanus* during an eight week growth trial. Impaired protein utilization is corroborated by lower post prandial ammonia efflux (indicator of protein catabolism), and more intact faeces with a higher protein content (poor protein digestions and/or absorption). The clear effects reported here of decreased protein and increased lipid contents contrast with knockout studies in tetrapods that did not find any changes. Appetite was unaffected as was brain satiation gene expression. The decreased SDA duration and lower intestinal CCK expression also suggest an increase in gastric emptying rates.

Impacts on post prandial metabolic rate

Our results showed a 21.8% decrease in the magnitude of SDA in *atp4a*$^{-/-}$ animals voluntarily fed a bloodworm meal relative to *atp4a*$^{+/+}$ fish. Although the animals in our study did not experience a decrease in growth, the reduction in postprandial ammonia excretion rates indicate reduced protein catabolism/digestion. Previous studies have reached varying conclusions on the impact of the decreased stomach acidification on SDA. In particular, Moffatt et al. (2022) estimated a decrease of 34.5% in the magnitude of the SDA in Nile tilapia treated with omeprazole. Goodrich et al. (2022a) estimated a value of 45% in magnitude reduction when barramundi (*Lates calcarifer*) were fed acidified diets that were expected to reduce the magnitude of proton pumping by HKA and increase growth efficiency (Lückstädt, 2008). Furthermore, in another study, Goodrich and co-workers (2022b) found that trout fed buffered diets that would lead to an increase in luminal proton pumping to acidify the chyme had an increase of 11% in SDA magnitude. These findings in teleosts contrast with results from studies in snakes that largely failed to detect a discernible impact on SDA (reviewed by Andrade et al., 2005; Henriksen et al., 2015; Nørgaard et al., 2016). The energetic costs of acid secretion and maintenance of the proton pump are thought to be relatively small and to not contribute a significant direct cost in snakes (Wang & Rindom, 2021). To address this discrepancy, in *A. mexicanus* we estimated the metabolic cost of post-prandial gastric acid secretion by using

stomach and food pH differences (Ferreira et al. 2025b), food buffer capacity (Supplemental material) and meal size (5% BM) to determine acid secretion, and published H^+ secretion: Oxygen consumption ratios [5.0 and 2.3, Kopic et al. (2010) and Bannister (1965), respectively, with the latter taking into consideration inefficiencies because of proton back leak]. The calculated oxygen consumption rates are 0.564 and 1.226 µmol $O_2 \cdot g^{-1}$ BM. The proton pump acid secretion only accounts for 2.6-5.6% of SDA magnitude of WT fish compared to the 21.8% difference in WT versus KO fish. This relatively small direct cost of acid secretion indicates that the impact of the lack of stomach acidification on postprandial energy expenditure is substantially larger when considering its importance in protein digestion, assimilation, and growth. However, it should be kept in mind that there are also likely indirect costs such as mucus and HCO_3^- secretion (alkaline tide and chyme neutralization) that are not considered in these calculations (e.g. Goodrich et al. 2022b).

Additionally, the 11% decrease in the overall duration of the SDA in the *atp4a*$^{-/-}$ fish suggests a faster evacuation time (reduced digestive / absorptive period), which contributes to the overall decrease in SDA magnitude. Previous studies (Couturier et al. 2013, Andersen et al., 2016) positively correlated the buffering capacity of the diet with increased gut transit times, agreeing with the current study findings of a shorter SDA time in the absence of stomach acidification. Although we were unable to detect a faster evacuation, this may be explained for technical reasons. The fish were relatively small (~ 0.4 g in a species that reaches the 3 g range, Riddle et al. 2021), and thus so were the ingested amounts of feed, and the overall volume capacity of their stomachs that may mask any changes in gastric evacuation due to the lack of necessary resolution in the measurements. In contrast, in a study on much larger Nile tilapia (100 g range), a decrease of 34.4% in the duration of SDA had been previously reported in omeprazole treated tilapia and related to faster gastric evacuation rates (Moffatt et al., 2022). Future studies should repeat these measurements in larger *A. mexicanus* fed a variety of meal sizes and feed types with a marker to track transit times (Langton & Center, 1977). Importantly, allowing the fish to control intake (by supplying an unlimited amount of food) could

dramatically impact transit time more accurately. For example, in gastric bypass mice, the treatment animals ate more, had lower digestibility, and faster transit of material through the gut (Liou et al., 2013).

CCK and gastric emptying

An explanation for the poor digestion in *atp4a*$^{-/-}$ fish can be provided by the observed decrease in cck mRNA and Cck concentrations in the anterior intestine. The downregulation of *cck* is likely the result of the absence of a feedback mechanism in response to pH changes in the anterior intestine resulting from the entry of an acidic chyme into this portion of the intestinal tract (Goyal et al., 2019). In the *atp4a*$^{-/-}$ fish, that lack the capacity to acidify the chyme, the arrival of a non-acidic chyme to the intestine would not trigger a pH-mediated response that leads to the secretion of Cck into the bloodstream and consequent changes in stomach motility and decreased gastric emptying. In this way, this decrease in our Cck data is likely indicative of faster chyme transit from the stomach to the intestine. Importantly, naturally agastric species and herbivores are expected to have faster transit times that are accompanied by more frequent meal ingestion (German, 2009; Jumars, 2000). Thus, the current *atp4a*$^{-/-}$ model regarding food intake and satiation fits this pattern as well.

Digestion, assimilation and growth

Since gastric acid is essential for the activation of gastric proteases, a decreased level of protein digestion/metabolism was expected (Kageyama, 2002) as well as the lytic action of gastric acid (Moriarty 1973). Indeed, the analyses of the nutrient profile in the carcass of *A. mexicanus* revealed a decreased protein content in *atp4a*$^{-/-}$ fish. These results, combined with an increase in protein content in the faeces consisting of more intact blood worms, support the importance

of HKA in protein digestion and assimilation capacity. In agreement with the lower protein uptake and digestive capacity, we have observed significantly lower levels of postprandial ammonia excretion in *atp4a*$^{-/-}$ fish as well. Elevated plasma ammonia levels are produced during digestion from amino acid catabolism in the gut epithelium (Karlsson et al., 2006) and liver (Ip & Chew, 2010).

We also observed that the gastric chyme ammonia concentration was higher in *atp4a*$^{-/-}$ fish. Since the source of this ammonia in the gastric chyme can be accounted for by the ammonia originating in the ingested bloodworm meal, this difference indicates an impairment in the absorption of ammonia from the food by the gut of knockout fish. Our results support a role for the stomach in dietary ammonia absorption, which is consistent with the observation by Jung et al. (2023) in rainbow trout. The mechanism of gastric absorption remains to be defined (Fereira et al. 2025b). The unabsorbed dietary ammonia in *atp4a*$^{-/-}$ fish is likely excreted by the rectum in the faeces (Wood and Eom 2025). However, since fecal ammonia was not measured, its relative contribution to the elevated total nitrogen measured in feces is unknown.

Notably, our growth data contrast with the reported decrease in growth in Nile tilapia (*Oreochromis niloticus*) treated with the PPI omeprazole (Moffatt et al., 2022). More importantly, since both *atp4a*$^{+/+}$ and *atp4a*$^{-/-}$ fish grew at similar rates during the eight week growth trial, it was only when *A. mexicanus* were given a diet supplemented with the proton pump inhibitor omeprazole did both groups experience a decreased growth rate. This was accompanied by increased food conversion ratios that are indicative of a reduced ability to convert ingested food into growth. There were no apparent changes to appetite when fish were fed omeprazole supplemented feed (all fish ingested the entire meal within 3 h, similarly to observations with untreated feed). This effect persisted for the first few weeks after the return to a non-treated diet. These findings point to possible off-target effects of omeprazole that inhibit growth independently of acid secretion, since the *atp4a*$^{-/-}$ are achlorhydric already. In general omeprazole is noted as a specific HKA inhibitor because of the need for acidification to

activate the inhibitor (Huttunen et al., 2011), and there are relatively few side effects when prescribed to treat gastroesophageal reflux disease (GERD), gastric ulcers and gastric reflux (Schubert, 2019). However, off target effects have been reported although not without some controversy (Cartee & Wang, 2020; Perry et al., 2020). Of note, previous studies in sea urchin (*Strongylocentrotus purpuratus*) by Stumpp et al. (2015) showed an effect of omeprazole on gastric alkalization in echinoderm tornaria larvae, an organism that lacks the HKA altogether (Okamura et al., 2003), further corroborating the hypothesis of the existence of secondary targets of this drug. This is an important finding, as it reveals an off-target effect of omeprazole, raising important questions on possible secondary effects of this widely used drug. It is important to consider that a longer growth trial period may reveal long term impacts in growth rates that were not detected in the present study (e.g. Cohen-Rothschild et al. 2024). Notably, the *atp4a*$^{-/-}$ fish were significantly smaller at the end of the recovery period. However, these results could be, among other hypotheses, the result of the impact of the omeprazole diet in the gut microbiome and digestion capacity that may affect differently the two genotypes. These findings pose important questions regarding the modulation of the gut microbiome by omeprazole in the presence and absence of gastric acid, opening the way to further research.

The *atp4a*$^{-/-}$ fish had a higher lipid content which is a novel finding that has not been reported in any previous study of knockout or knockdown of HKA (Judd et al., 2005; Moffatt et al., 2022; Zhao et al., 2010). The analysis of the mineral content of the carcasses also revealed a decrease in phosphorus content. The phosphorus requirements of fish are met mainly through diet (NRC, 2011). Notably, phosphorus is found in fish meal as hydroxyapatite (an insoluble Ca–P complex), and increased availability has been linked to acid hydrolysis (Albrektsen et al., 2018; NRC, 2011; Sugiura et al., 2006). This agrees with our data; whereby gastric acid secretion plays an important role in the solubilization of phosphate from the diet. In contrast, aquaculture feed companies often improve digestibility by supplementing diets with inorganic phosphorous salts (Hua and Bureau 2006). Significantly, previous studies (Abuduli et al., 2016; Chun et al., 2016; Wong, 2022; Zhang et al., 2023) have also established the importance of phosphorus in the

regulation of body lipid content, through regulation of lipid biosynthesis and oxidation pathways. In this way, the increase in body fat observed in *atp4a*$^{-/-}$ fish in this study is likely related to phosphorus malabsorption. In addition, the presence of phosphorus is important for calcium regulation (Taylor & Bushinsky, 2009). Calcium and phosphorus are of critical importance in the development and maintenance of skeletal function, among other physiological functions related to acid-base homeostasis (Fontagné et al., 2009; Lall & Kaushik, 2021; Zimmer et al., 2019). Indeed, our results show a decrease in carcass calcium content in *atp4a*$^{-/-}$ fish as well. Future research should aim to determine changes in bone density and to explore possible changes in the skeleton at earlier stages of development.

Our findings are consistent with reports of hypomagnesaemia under pharmacological knockdown of the proton pump with proton pump inhibitor (PPI) administration (Jaworek, 2020; Judd et al., 2005; Schubert, 2019; Zhao et al., 2010). Magnesium is a divalent cation that plays an essential role in the physiological processes of protein synthesis, cell replication, and energy metabolism and, in bony fishes, 50-70% or more is stored in skeletal tissues and scales (Bijvelds et al., 1998, Lall & Kaushik, 2021) in contrast to 99% of calcium and 80% of phosphorous (FAO 1980). The magnesium requirement for fish is mainly achieved through diet and several mechanisms for intestinal transcellular magnesium uptake have been identified in teleosts [*slc41a1, trpm6*, (Arjona et al., 2019; Kodzhahinchev et al., 2017)]. Further studies are needed to investigate the causes of the significant decrease in Mg body content in *atp4a*$^{-/-}$ fish and possible links to decreased transcellular Mg^{2+} transport.

Alkaline tide

When acid is secreted into the stomach lumen, the base that is generated makes its way into the blood stream as the alkaline tide (Brunton, 1933; Niv & Fraser, 2002). The small size of the fish precluded the possibility of measuring the alkaline tide directly in the blood, but it might be

observable as an increase in the whole animal base flux into the water (Wood 2019). However, the predicted postprandial alkaline tide in the blood did not translate to an increase in base efflux in *atp4a*$^{+/+}$ animals. Instead, within the first 24 h after feeding, net acid excretion is observed in *atp4a*$^{+/+}$ fish, corresponding to base uptake, while the net base excretion is not different from zero in *atp4a*$^{-/-}$ animals. This is likely due to the nature of the meal and the small ration size fed to the animals (5 % BM wet blood worms ~ 1% BM dry bloodworm) that may be insufficient to produce substantial base excretion into the water (Wood, 2019). Our findings are comparable to those obtained by Cooper and Wilson (2008), who showed a negligible net base excretion in rainbow trout fed a 1% BM meal of pellets, which contrasts with observations of a substantial flux in rainbow trout fed a larger 5% BM meal (Bucking & Wood, 2008) and in barramundi fed a 2.5% BM ration (Goodrich et al., 2022b). Another relevant component at play in the interpretation of these data is the large increase in ammonia excretion. Thus, although these data do not support the existence of a postprandial base excretion in *A. mexicanus* fed a 5% BM wet bloodworm meal, the significant decrease in ammonia excretion in *atp4a*$^{+/+}$ is likely driving the differences seen in net acid-base flux between the two groups.

Conclusions

Our study addresses long-standing physiological questions in gastrointestinal physiology with resource to a genetic knockout of the gastric proton pump. This approach reduces confounding factors that may arise from indirect gastric modulation methods. Taken together, the lower protein digestibility, lower ammonia metabolism, and possible changes to gut transit times, further support the changes in SDA in HKA-null animals reported in this study. In previous studies of HKA modulation (Secor, 2009; Moffatt et al., 2022; Goodrich et al., 2022a, 2022b), and from our own findings it is clear the HKA importance transcends the direct cost of acidification and are likely related to changes in nutrient assimilation caused by the absence of acid (Goodrich et al., 2024). This study is the first to report a significant depletion in ammonia

excretion rates following inhibition/ablation of HKA in vertebrates. Conclusions should, however, be made cautiously since the animals in this study were fed a high protein diet and the same trend may not be noticed with different food sources. We have linked a decrease in acidification to a reduced SDA, in agreement with previous studies, but no decrease in growth efficiency. We expect that the knockout of gastric acid in an obligate carnivore species would produce a notable effect in growth rates since it is clear the absence of gastric acidification precludes an efficient digestion of proteins. We have established a direct link between gastric acid secretion and magnesium, calcium and phosphate balance in Astyanax *mexicanus*. This new knockout line offers a good model for the study of mineral bone diseases, representing an advantage over currently used fish models that are agastric (Lleras-Forero et al., 2020) since it enables a direct comparison of different bone phenotypes within the same species. Lastly, these findings offer new insights into the importance of the stomach as an evolutionary innovation in gnathostomes, while opening the way for a better understanding of the physiological pressures and demands of the secondary loss events of this organ in numerous vertebrate clades.

Acknowledgements

The authors would like to acknowledge the technical support and expertise of Gena Braun (Wilfrid Laurier University) which was essential to the ICP and CHN analyses. We would also like to thank the two anonymous reviewers for their constructive comments and suggestions, and to Dr. R.W. Wilson for discussions on the metabolic costs of acidification.

Data availability

Data can be accessed in the repository 10.5281/zenodo.17136376

Funding

This work was funded by grants from the Natural Sciences and Engineering Research Council of Canada (NSERC)-Discovery RGPIN-2019-06838 to J.M.W., Canadian Foundation for Innovation John R. Evans Leaders Fund (JELF) No. 32713 Grant to J.M.W., and Ontario Graduate Scholarships (OGS 2020, 2021, 2023) to P.G.F.

Disclosures

No conflicts of interest, financial or otherwise, are declared by the authors.

References

Abuduli, M., Ohminami, H., Otani, T., Kubo, H., Ueda, H., Kawai, Y., Masuda, M., Yamanaka-Okumura, H., Sakaue, H., Yamamoto, H., & others. (2016). Effects of dietary phosphate on glucose and lipid metabolism. *American Journal of Physiology-Endocrinology and Metabolism*, *310*(7), E526–E538.

Albrektsen, S., Lock, E.-J., Bæverfjord, G., Pedersen, M., Krasnov, A., Takle, H., Veiseth-Kent, E., Ørnsrud, R., Waagbø, R., & Ytteborg, E. (2018). Utilization of $H_2SO_4^-$ hydrolysed phosphorus from herring bone by-products in feed for Atlantic salmon (*Salmo salar*) 0+ postsmolt. *Aquaculture Nutrition*, *24*(1), 348–365.

Andersen, N. G., Chabot, D. & Couturier, C. S. (2016) Modelling gastric evacuation in gadoids feeding on crustaceans. *J. Fish Biol* 88, 1886-1903 Andrade, D., Abe, A., Cruz-Neto, A., & Wang, T. (2005). Specific dynamic action in ectothermic vertebrates: A general review on the determinants of the metabolic responses to digestion in fish, amphibians and reptiles. *Adaptations in Food Processing and Digestion in Vertebrates. Science Publishers Inc*, 305–324.

Arjona, F. J., Latta, F., Mohammed, S. G., Thomassen, M., van Wijk, E., Bindels, R. J., Hoenderop, J. G., & de Baaij, J. H. (2019). SLC41A1 is essential for magnesium homeostasis in vivo. *Pflügers Archiv-European Journal of Physiology*, *471*, 845–860.

Aspiras, A. C., Rohner, N., Martineau, B., Borowsky, R. L., & Tabin, C. J. (2015). Melanocortin 4 receptor mutations contribute to the adaptation of cavefish to nutrient-poor conditions. *Proceedings of the National Academy of Sciences of the United States of America*, *112*(31), 9668–9673. https://doi.org/10.1073/pnas.1510802112

Beamis, F., Nijmi, A., & Lett, P. (1975). Bioenergetics of teleost fishes: Environmentalinfluences. Comparative Physiology-Functional Aspects of Structural Materials. *Comparative Physiology: Functional Aspects of Structural Materials: Proceedings of the International Conference on Comparative Physiology, Ascona, 1974*, *2*, 187.

Bijvelds, M.J., Van Der Velden, J.A., Kolar, Z.I. and Flik, G., (1998). Magnesium transport in freshwater teleosts. *Journal of Experimental Biology*, 201(13), 1981-1990.

Brown, C. R., & Cameron, J. N. (1991a). The induction of specific dynamic action in channel catfish by infusion of essential amino acids. *Physiological Zoology*, *64*(1), 276–297.

Brown, C. R., & Cameron, J. N. (1991b). The relationship between specific dynamic action (SDA) and protein synthesis rates in the channel catfish. *Physiological Zoology*, *64*(1), 298–309.

Brunton, C. E. (1933). The acid output of the kidney and the so-called alkaline tide. *Physiological Reviews*, *13*(3), 372–399.

Bucking, C., Fitzpatrick, J. L., Nadella, S. R., & Wood, C. M. (2009). Post-prandial metabolic alkalosis in the seawater-acclimated trout: The alkaline tide comes in. *Journal of Experimental Biology*, *212*(14), 2159–2166. https://doi.org/10.1242/jeb.027862

Cameron, J. N., & Heisler, N. (1983). Studies of Ammonia in the Rainbow Trout Physico-Chemical Parameters, Acid-Base Behaviour and Respiratory Clearance. *Journal of Experimental Biology*, *105*(1), 107–125.

Cartee, N. M. P., & Wang, M. M. (2020). Binding of omeprazole to protein targets identified by monoclonal antibodies. *PloS One*, *15*(9), e0239464.

Castro, L., Gonçalves, O., Mazan, S., Tay, B., Venkatesh, B., & Wilson, J. M. (2014). Recurrent gene loss correlates with the evolution of stomach phenotypes in gnathostome history. *Proceedings of the Royal Society of London B*: *Biological Sciences*, 281 (1775), 20132669.

Chabot, D., Koenker, R., & Farrell, A. (2016). The measurement of specific dynamic action in fishes. *Journal of Fish Biology*, *88*(1), 152–172.

Chandel, N.S., (2021). Amino acid metabolism. Cold Spring Harbor perspectives in biology, 13(4), a040584.

Chun, S., Bamba, T., Suyama, T., Ishijima, T., Fukusaki, E., Abe, K., & Nakai, Y. (2016). A high phosphorus diet affects lipid metabolism in rat liver: A DNA microarray analysis. *PloS One*, *11*(5), e0155386.

Cohen-Rothschild, N., Mizrahi, N. and Levavi-Sivan, B. (2024). Characterization of a novel fast-growing zebrafish: a new approach to growth hormone transgenesis. *Frontiers in Endocrinology*, *15*, 1369043.

Cooper, C. A., & Wilson, R. W. (2008). Post-prandial alkaline tide in freshwater rainbow trout: Effects of meal anticipation on recovery from acid–base and ion regulatory disturbances. *Journal of Experimental Biology*, *211*(15), 2542–2550. https://doi.org/10.1242/jeb.015586

Corp, E. S., McQuade, J., Moran, T. H., & Smith, G. P. (1993). Characterization of type A and type B CCK receptor binding sites in rat vagus nerve. *Brain Research*, *623*(1), 161–166.

Crane, D. P., Ogle, D. H., & Shoup, D. E. (2020). Use and misuse of a common growth metric: Guidance for appropriately calculating and reporting specific growth rate. *Reviews in Aquaculture*, *12*(3), 1542–1547.

Couturier, C. S., Andersen, N. G., Audet, C. & Chabot, D. (2013) Prey exoskeletons influence the course of gastric evacuation in Atlantic cod *Gadus morhua*. *J. Fish Biol* 82, 789-805 .

FAO (Food And Agriculture Organization) of the United Nations (1980). Fish Feed Technology (ADCP/REP/80/11). FAO Rome.

Ferreira, P. G., Castro, L. F. C., & Wilson, J. M. (2025a). A second look at the stomach–a fishy perspective. *Journal of Experimental Biology*, *228*(14), jeb250054.

Ferreira, P. G., Vogl, A. W., Castro, L. F. C., & Wilson, J. M. (2025b). Generation of gastric proton pump *atp4a* knockouts in *Astyanax mexicanus*: A fish model for insights into the mechanisms of acidification by oxynticopeptic cells. *American Journal of Physiology-Gastrointestinal and Liver Physiology*, *329*(1), G88–G101.

Flávio, H. (2025). pyroresp: Analyse respirometry data captured by firesting loggers. https://github.com/hugomflavio/pyroresp

Fontagné, S., Silva, N., Bazin, D., Ramos, A., Aguirre, P., Surget, A., Abrantes, A., Kaushik, S. J., & Power, D. M. (2009). Effects of dietary phosphorus and calcium level on growth and skeletal development in rainbow trout (*Oncorhynchus mykiss*) fry. *Aquaculture*, *297*(1–4), 141–150.

Fu, S., Xie, X., & Cao, Z. (2005). Effect of meal size on postprandial metabolic response in southern catfish (*Silurus meridionalis*). *Comparative Biochemistry and Physiology Part A: Molecular & Integrative Physiology*, *140*(4), 445–451.

German, D. P. (2009). Do herbivorous minnows have "plug-flow reactor" guts? Evidence from digestive enzyme activities, gastrointestinal fermentation, and luminal nutrient concentrations. *Journal of Comparative Physiology B*, *179*(6), 759–771.

Goodrich, H. R., Berry, A. A., Montgomery, D. W., Davison, W. G., & Wilson, R. W. (2022a). Fish feeds supplemented with calcium-based buffering minerals decrease stomach acidity, increase the blood alkaline tide and cost more to digest. *Scientific Reports*, *12*(1), 18468.

Goodrich, H. R., Wilson, R. W., Smullen, R., Barnes, A. C., & Franklin, C. E. (2022b). Acidified fish feeds reduce the energetic and physiological costs of digestion in juvenile barramundi (*Lates calcarifer*). *Aquaculture*, *546*, 737400. https://doi.org/10.1016/j.aquaculture.2021.737400

Goodrich, H. R., Wood, C. M., Wilson, R. W., Clark, T. D., Last, K. B., & Wang, T. (2024). Specific dynamic action: The energy cost of digestion or growth? *Journal of Experimental Biology*, *227*(7), jeb246722.

Goyal, R. K., Guo, Y., & Mashimo, H. (2019). Advances in the physiology of gastric emptying. *Neurogastroenterology & Motility*, *31*(4), e13546.

Henriksen, P. S., Enok, S., Overgaard, J., & Wang, T. (2015). Food composition influences metabolism, heart rate and organ growth during digestion in *Python regius*. *Comparative Biochemistry and Physiology Part A: Molecular & Integrative Physiology*, *183*, 36–44.

Holmgren, S., & Holmberg, A. (2005). Control of gut motility and secretion in fasting and fed non-mammalian vertebrates. In J. M. Starck & T. Wang (Eds.), *Physiological and ecological adaptations to feeding in vertebrates. Science Publishers, New Hampshire* (pp. 107–123). Science Pub Inc.

Holstein, B. (1982). Inhibition of gastric acid secretion in the Atlantic cod, *G*adus morhua, by sulphated and desulphated gastrin, caerulein, and CCK-octapeptide. *Acta Physiologica Scandinavica*, *114*(3), 453–459.

Houlihan, D.F., Pannevis, M. and Heba, H. (1993). Protein synthesis in juvenile tilapia *Oreochromis mossambicus*. *Journal of the World Aquaculture Society*, *24*(2), 145-151.

Hua, K. and Bureau, D.P. (2006). Modelling digestible phosphorus content of salmonid fish feeds. Aquaculture, 254(1-4), 455-465.

Huttunen, K. M., Raunio, H., & Rautio, J. (2011). Prodrugs—From serendipity to rational design. *Pharmacological Reviews*, *63*(3), 750–771.

Imarazene, B. (2020). *Microévolution des déterminismes sexuels chez le poisson Tétra Mexicain, Astyanax mexicanus* [PhD Thesis]. Université de Rennes.

Ip, Y. K., & Chew, S. F. (2010). Ammonia production, excretion, toxicity, and defense in fish: A review. *Frontiers in Physiology*, *1*, 134.

Jaworek, A. J. (2020). Proton Pump Inhibitor Controversies. *Laryngopharyngeal and Gastroesophageal Reflux: A Comprehensive Guide to Diagnosis, Treatment, and Diet-Based Approaches*, 285–323.

Jones, H. B. (1845). XV. Contributions to the chemistry of the urine. On the variations in the alkaline and earthy phosphates in the healthy state, and on the alkalescence of the urine from fixed alkalies. *Philosophical Transactions of the Royal Society of London*, *135*, 335–349.

Judd, L. M., Andringa, A., Rubio, C. A., Spicer, Z., Shull, G. E., & Miller, M. L. (2005). Gastric achlorhydria in H/K-ATPase-deficient (Atp4a(–/–)) mice causes severe hyperplasia, mucocystic metaplasia and upregulation of growth factors. *Journal of Gastroenterology and Hepatology*, *20*(8), 1266–1278. https://doi.org/10.1111/j.1440-1746.2005.03867.x

Jumars, P. A. (2000). Animal Guts as Ideal Chemical Reactors: Maximizing Absorption Rates. *The American Naturalist*, *155*(4), 527–543. https://doi.org/10.1086/303333

Jung, E. H., Brauner, C. J., & Wood, C. M. (2023). Do extreme postprandial levels of oxygen, carbon dioxide, and ammonia in the digestive tract equilibrate with the bloodstream in the freshwater rainbow trout (*Oncorhynchus mykiss*)? *Journal of Comparative Physiology B*, *193*(2), 193–205. https://doi.org/10.1007/s00360-023-01475-8

Kageyama, T. (2002). Pepsinogens, progastricsins, and prochymosins: Structure, function, evolution, and development. *Cellular and Molecular Life Sciences CMLS*, *59*(2), 288–306. https://doi.org/10.1007/s00018-002-8423-9

Karlsson, A., Eliason, E. J., Mydland, L. T., Farrell, A. P., & Kiessling, A. (2006). Postprandial changes in plasma free amino acid levels obtained simultaneously from the hepatic portal vein and the dorsal aorta in rainbow trout (*Oncorhynchus mykiss*). *Journal of Experimental Biology*, *209*(24), 4885–4894.

Kato, A., Pipil, S., Ota, C., Kusakabe, M., Watanabe, T., Nagashima, A., Chen, A.-P., Islam, Z., Hayashi, N., Wong, M. K.-S., Komada, M., Romero, M., & Takei, Y. (2024). Convergent gene losses and pseudogenizations in multiple lineages of stomachless fishes. *Communications Biology,* 7 (1), 408.

Kaushik, S. J., & de Oliva Teles, A. (1985). Effect of digestible energy on nitrogen and energy balance in rainbow trout. *Aquaculture*, *50*(1), 89–101. https://doi.org/10.1016/0044-8486(85)90155-3

Kodzhahinchev, V., Kovacevic, D., & Bucking, C. (2017). Identification of the putative goldfish (*Carassius auratus*) magnesium transporter SLC41a1 and functional regulation in the gill, kidney, and intestine in response to dietary and environmental manipulations. *Comparative Biochemistry and Physiology Part A: Molecular & Integrative Physiology*, *206*, 69–81.

Koelz, H. R. (1992). Gastric Acid in Vertebrates. *Scandinavian Journal of Gastroenterology*, *27*(sup193), 2–6. https://doi.org/10.3109/00365529209095998

Kopic, S., Murek, M., & Geibel, J. P. (2010). Revisiting the parietal cell. *American Journal of Physiology. Cell Physiology*, *298*(1), C1–C10. https://doi.org/10.1152/ajpcell.00478.2009

Lall, S. P., & Kaushik, S. J. (2021). Nutrition and metabolism of minerals in fish. *Animals*, *11*(09), 2711.

Langton, R. W., & Center, N. (1977). A review of methods used for estimating gut evacuation rates and calculating daily ration for fish. *Ref. Doc*, 77–07.

Lin, C., & Miller, T. R. (1992). Both CCK-A and CCK-B/gastrin receptors are present on rabbit vagus nerve. *American Journal of Physiology-Regulatory, Integrative and Comparative Physiology*, *263*(3), R591–R595.

Liou, A. P., Paziuk, M., Luevano Jr, J.-M., Machineni, S., Turnbaugh, P. J., & Kaplan, L. M. (2013). Conserved shifts in the gut microbiota due to gastric bypass reduce host weight and adiposity. *Science Translational Medicine*, *5*(178), 178ra41-178ra41.

Livak, K. J., & Schmittgen, T. D. (2001). Analysis of Relative Gene Expression Data Using Real-Time Quantitative PCR and the 2−ΔΔCT Method. *Methods*, *25*(4), 402–408. https://doi.org/10.1006/meth.2001.1262

Lleras-Forero, L., Winkler, C., & Schulte-Merker, S. (2020). Zebrafish and medaka as models for biomedical research of bone diseases. *Developmental Biology*, *457*(2), 191–205.

Lückstädt, C. (2008). Effect of dietary potassium diformate on the growth and digestibility of Atlantic salmon *Salmo salar*. *Proceedings of the 13th International Symposium on Fish Nutrition & Feeding, Florianopolis, Brazil*, 279.

Lyndon, A. R., Houlihan, D. F., & Hall, S. (1992). The effect of short-term fasting and a single meal on protein synthesis and oxygen consumption in cod, *Gadus morhua*. *Journal of Comparative Physiology B*, *162*(3), 209–215.

Mariotti, F., Tomé, D. and Mirand, P.P. (2008). Converting nitrogen into protein—beyond 6.25 and Jones' factors. *Critical Reviews in Food Science and Nutrition 48*(2), 177-184.

McDonald, D., & Wood, C. (1981). Branchial and renal acid and ion fluxes in the rainbow trout, *Salmo gairdneri*, at low environmental pH. *Journal of Experimental Biology*, *93*(1), 101–118.

Moffatt, K., Rossi, M., Park, E., Svendsen, J. C., & Wilson, J. M. (2022). Inhibition of gastric acid secretion with omeprazole affects fish specific dynamic action and growth rate: Implications for the development of phenotypic stomach loss. *Frontiers in Physiology*, *13*, 966447.

Niv, Y., & Fraser, G. M. (2002). The alkaline tide phenomenon. *Journal of Clinical Gastroenterology*, *35*(1), 5–8.

Nørgaard, S., Andreassen, K., Malte, C. L., Enok, S., & Wang, T. (2016). Low cost of gastric acid secretion during digestion in ball pythons. *Comparative Biochemistry and Physiology Part A: Molecular & Integrative Physiology*, *194*, 62–66.

NRC. (2011). *Nutrient requirements of fish and shrimp*. National Academies Press.

Okamura, H., Yasuhara, J. C., Fambrough, D. M., & Takeyasu, K. (2003). P-type ATPases in Caenorhabditis and Drosophila: Implications for Evolution of the P-type ATPase Subunit Families with Special Reference to the Na,K-ATPase and H,K-ATPase Subgroup. *Journal of Membrane Biology*, *191*(1), 13–24. https://doi.org/10.1007/s00232-002-1041-5

Olsson, C., Aldman, G., Larsson, A., & Holmgren, S. (1999). Cholecystokinin affects gastric emptying and stomach motility in the rainbow trout *Oncorhynchus mykiss*. *Journal of Experimental Biology*, *202*(2), 161–170.

Perry, I. E., Sonu, I., Scarpignato, C., Akiyama, J., Hongo, M., & Vega, K. J. (2020). Potential proton pump inhibitor–related adverse effects. *Annals of the New York Academy of Sciences*, *1481*(1), 43–58.

Richter, C., Tanaka, T., & Yada, R. Y. (1998). Mechanism of activation of the gastric aspartic proteinases: Pepsinogen, progastricsin and prochymosin. *Biochemical Journal*, *335*(3), 481–490. https://doi.org/10.1042/bj3350481

Ricker, W. (1975). Computation and interpretation of biological statistics of fish populations. *Bulletin of the Fisheries Research Board of Canada*, *191*, 1–382.

Riddle, M.R., Aspiras, A., Damen, F., McGaugh, S., Tabin, J.A. and Tabin, C.J. (2021). Genetic mapping of metabolic traits in the blind Mexican cavefish reveals sex-dependent quantitative trait loci associated with cave adaptation. BMC ecology and evolution, 21(1), p.94.

Rubino, J. G., Zimmer, A. M., & Wood, C. M. (2014). An in vitro analysis of intestinal ammonia handling in fasted and fed freshwater rainbow trout (*Oncorhynchus mykiss*). *Journal of Comparative Physiology B*, *184*(1), 91–105. https://doi.org/10.1007/s00360-013-0781-0

Schubert, M. L. (2019). Proton pump inhibitors: Placing putative adverse effects in proper perspective. *Current Opinion in Gastroenterology*, *35*(6), 509–516.

Secor, S. M. (2009). Specific dynamic action: A review of the postprandial metabolic response. *Journal of Comparative Physiology B*, *179*(1), 1–56.

Shin, J. M., Munson, K., Vagin, O., & Sachs, G. (2009). The gastric HK-ATPase: Structure, function, and inhibition. *Pflügers Archiv-European Journal of Physiology*, *457*(3), 609–622.

Shin, J. M., & Sachs, G. (2008). Pharmacology of proton pump inhibitors. *Current Gastroenterology Reports*, *10*(6), 528–534.

Smit, H. (1968). Gastric secretion in the lower vertebrates and birds. *Handbook of Physiology*, *5*(6), 135.

Smith, & Houlihan, D. (1995). Protein synthesis and oxygen consumption in fish cells. *Journal of Comparative Physiology B*, *165*, 93–101.

Smith, Moran, T. H., Coyle, J. T., Kuhar, M., O'Donahue, T., & McHugh, P. R. (1984). Anatomic localization of cholecystokinin receptors to the pyloric sphincter. *American Journal of Physiology-Regulatory, Integrative and Comparative Physiology*, *246*(1), R127–R130.

Stumpp, M., Hu, M. Y., Tseng, Y.-C., Guh, Y.-J., Chen, Y.-C., Yu, J.-K., Su, Y.-H., & Hwang, P.-P. (2015). Evolution of extreme stomach pH in bilateria inferred from gastric alkalization mechanisms in basal deuterostomes. *Scientific Reports*, *5*(1), 10421. https://doi.org/10.1038/srep10421

Sugiura, S. H., Roy, P. K., & Ferraris, R. P. (2006). Dietary acidification enhances phosphorus digestibility but decreases H^+/K^+-ATPase expression in rainbow trout. *Journal of Experimental Biology*, *209*(19), 3719–3728. https://doi.org/10.1242/jeb.02436

Swaminathan, A., Xia, F., & Rohner, N. (2024). From darkness to discovery: Evolutionary, adaptive, and translational genetic insights from cavefish. *Trends in Genetics*, *40*(1), 24–38. https://doi.org/10.1016/j.tig.2023.10.002

Taylor, J. G., & Bushinsky, D. A. (2009). Calcium and phosphorus homeostasis. *Blood Purification*, *27*(4), 387–394.

Taylor, J.R., Cooper, C.A. and Mommsen, T.P. (2010). Implications of GI function for gas exchange, acid–base balance and nitrogen metabolism. In *Fish Physiology* (Vol. 30, pp. 213-259). Academic Press.

Verdouw, H., Van Echteld, C., & Dekkers, E. (1978). Ammonia determination based on indophenol formation with sodium salicylate. *Water Research*, *12*(6), 399–402.

Volkoff, H., Canosa, L. F., Unniappan, S., Cerdá-Reverter, J. M., Bernier, N. J., Kelly, S. P., & Peter, R. E. (2005). Neuropeptides and the control of food intake in fish. *General and Comparative Endocrinology*, *142*(1), 3–19. https://doi.org/10.1016/j.ygcen.2004.11.001

Wang, T., & Rindom, E. (2021). The physiological response to digestion in snakes: A feast for the integrative physiologist. *Comparative Biochemistry and Physiology Part A: Molecular & Integrative Physiology*, *254*, 110891.

Wong, S. K. (2022). A review of current evidence on the relationship between phosphate metabolism and metabolic syndrome. *Nutrients*, *14*(21), 4525.

Wood, C. M. (2019). Internal spatial and temporal CO_2 dynamics: Fasting, feeding, drinking, and the alkaline tide. In M. Grosell, P. Munday, A. Farrell, & C. Brauner (Eds.), *Fish Physiology* (Vol. 37, pp. 245–286). Elsevier.

Wood, C. M., Bucking, C., Fitzpatrick, J., & Nadella, S. (2007). The alkaline tide goes out and the nitrogen stays in after feeding in the dogfish shark, *Squalus acanthias*. *Respiratory Physiology & Neurobiology*, *159*(2), 163–170. https://doi.org/10.1016/j.resp.2007.06.008

Wood, C.M. and Eom, J. (2025). Accounting for the role of the gastro-intestinal tract in the ammonia and urea nitrogen dynamics of freshwater rainbow trout on long-term satiation feeding. *Journal of Experimental Biology*, 228(14), jeb249654.

Wood, C. M., Schultz, A. G., Munger, R. S., & Walsh, P. J. (2009). Using omeprazole to link the components of the post-prandial alkaline tide in the spiny dogfish, *Squalus acanthias*. *Journal of Experimental Biology*, *212*(5), 684–692. https://doi.org/10.1242/jeb.026450

Xiong, S., Wang, W., Kenzior, A., Olsen, L., Krishnan, J., Persons, J., Medley, K., Peuß, R., Wang, Y., Chen, S., Zhang, N., Thomas, N., Miles, J. M., Alvarado, A. S., & Rohner, N. (2022). Enhanced lipogenesis through Pparγ helps cavefish adapt to food scarcity. *Current Biology: CB*, *32*(10), 2272-2280.e6. https://doi.org/10.1016/j.cub.2022.03.038

Zhang, M., Zhu, L., Wu, G., Zhang, H., Wang, X., & Qi, X. (2023). The impacts and mechanisms of dietary proteins on glucose homeostasis and food intake: A pivotal role of gut hormones. *Critical Reviews in Food Science and Nutrition*, 1–15.

Zhao, Z., Hou, N., Sun, Y., Teng, Y., & Yang, X. (2010). Atp4b promoter directs the expression of Cre recombinase in gastric parietal cells of transgenic mice. *Journal of Genetics and Genomics*, *37*(9), 647–652.

Zimmer, A. M., Brix, K. V., & Wood, C. M. (2019). Mechanisms of Ca^{2+} uptake in freshwater and seawater-acclimated killifish, *Fundulus heteroclitus*, and their response to acute salinity transfer. *Journal of Comparative Physiology B*, *189*, 47–60.

Figures and Tables

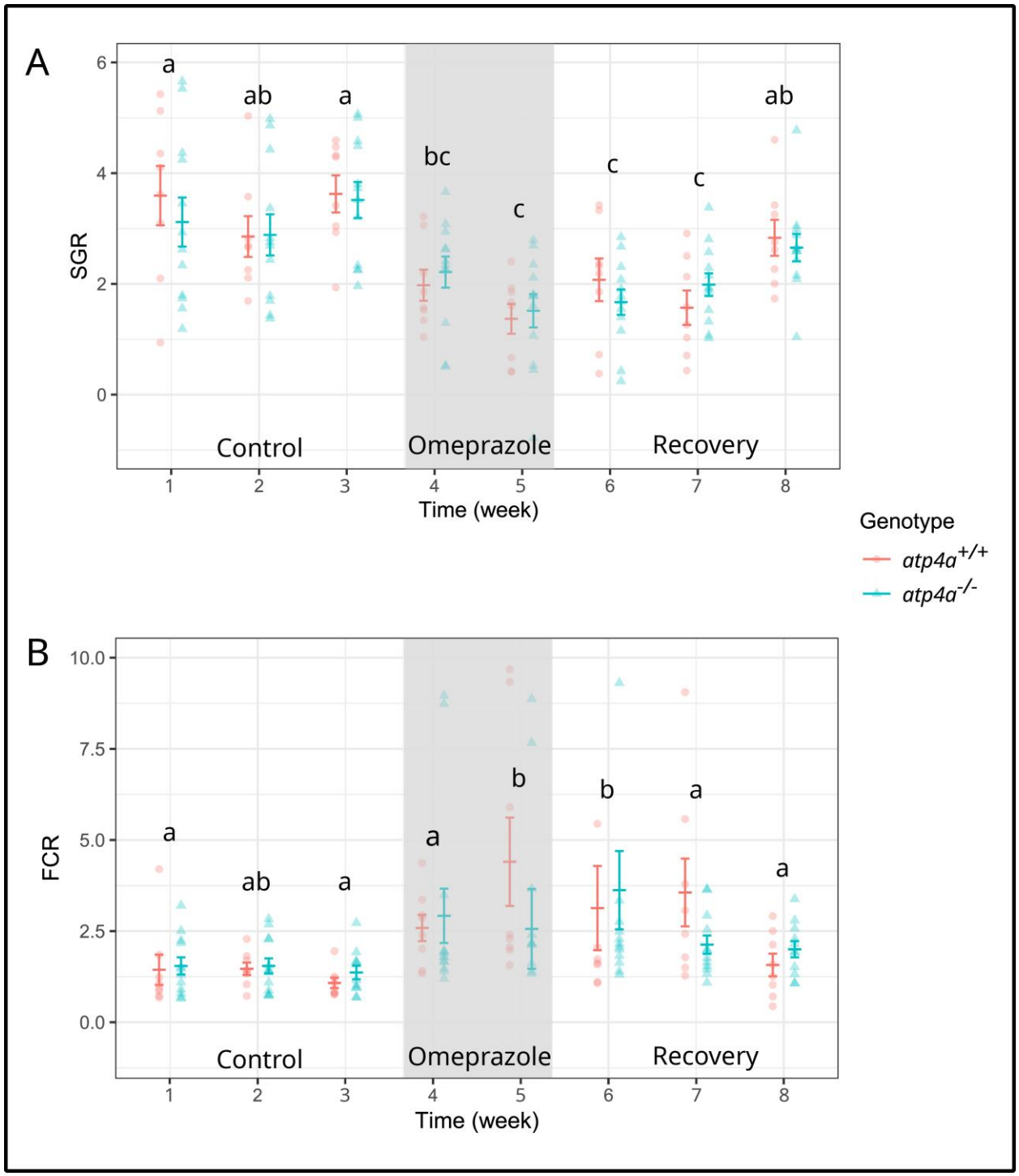

Fig. 1. *Astyanax mexicanus* growth trial. Both *atp4a*$^{+/+}$ and *atp4a*$^{-/-}$ animals were fed a 3% body-mass ration of pellets. In the first three weeks, both groups were fed regular (non-treated pellets). On weeks 4 and 5, both groups were fed the same ration size of pellets dosed with omeprazole (25mg kg^{-1} BM day^{-1}). Weeks 6-8 were recovery weeks (post-omeprazole), where both groups were fed untreated pellets. Animals were weighed every week throughout the trial period. Specific growth rates (SGR, **A**) and feed conversion ratios (FCR, **B**) were calculated over these weekly intervals. Data were analyzed by two-way ANOVA with Tukey posthoc test; n = 8 *atp4a*$^{+/+}$ and 12 *atp4a*$^{-/-}$. There were no significant differences nor interactions between genotypes. Significant differences were noted between trial weeks. The time intervals labelled with different letters are significantly different from each other, p-value < 0.05.

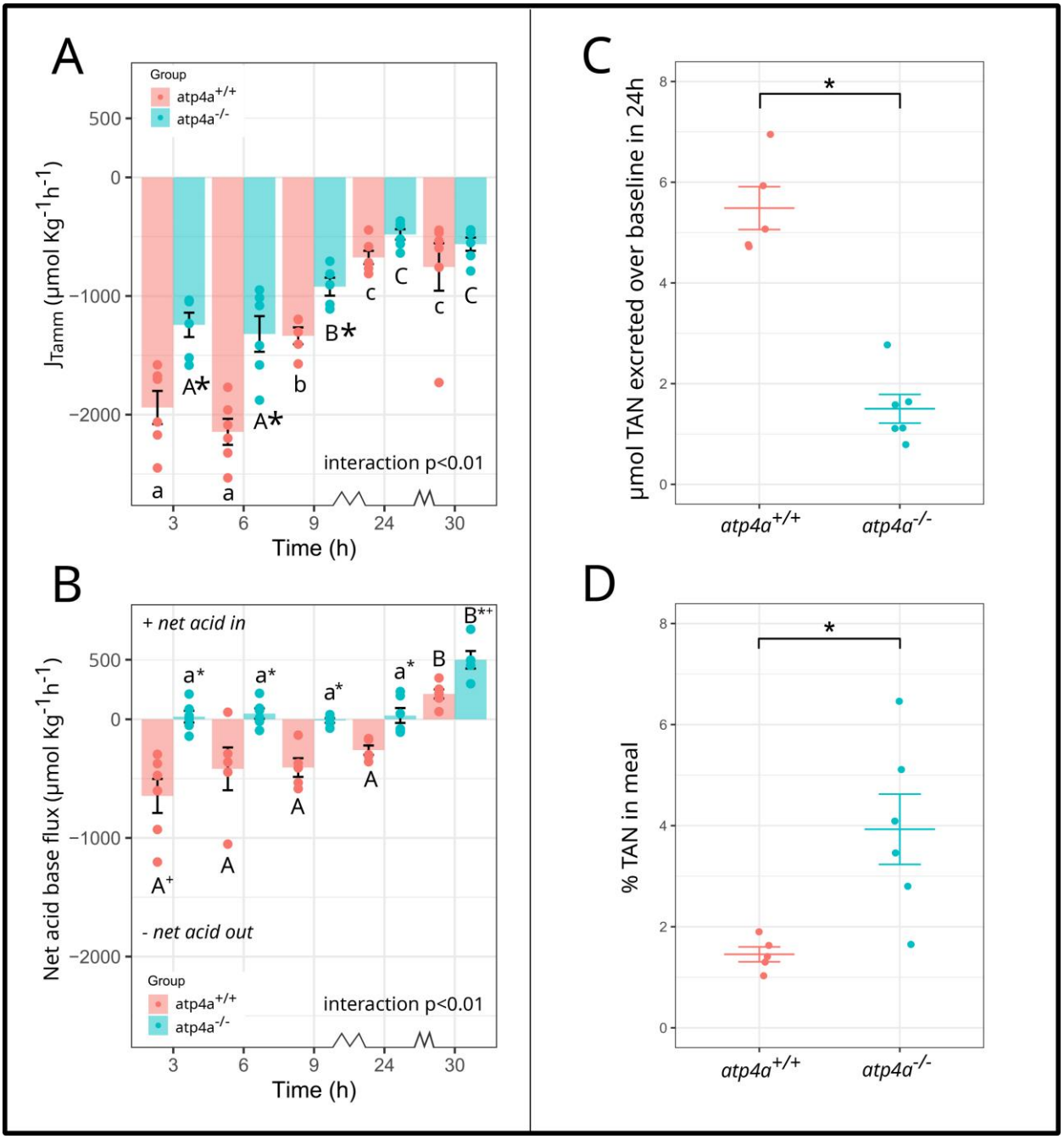

Fig. 2. Fluxes rates (µmol kg^{-1} body mass h^{-1}) of (**A**) ammonia and (**B**) net acid net acid (H^+) or base (OH^-) of *A. mexicanus atp4a*$^{+/+}$ and *atp4a*$^{-/-}$ fed a 5% ration of bloodworms (n = 8 per group). Negative values indicate a net base uptake (i.e. acid excretion) and positive values indicate net base excretion (i.e. acid uptake). Different letters indicate differences relative to 3h post-feed excretion. In panel **B**, superscript + indicates fluxes significantly different from 0. Data

are presented as mean ± SEM. **C** Cumulative ammonia (μmol) excreted over baseline per group. **D** Percentage of excreted ammonia corresponding to direct absorption from food ammonia, i.e. excluding feed catabolism. Significant differences ($p < 0.05$) between genotypes are identified by asterisks.

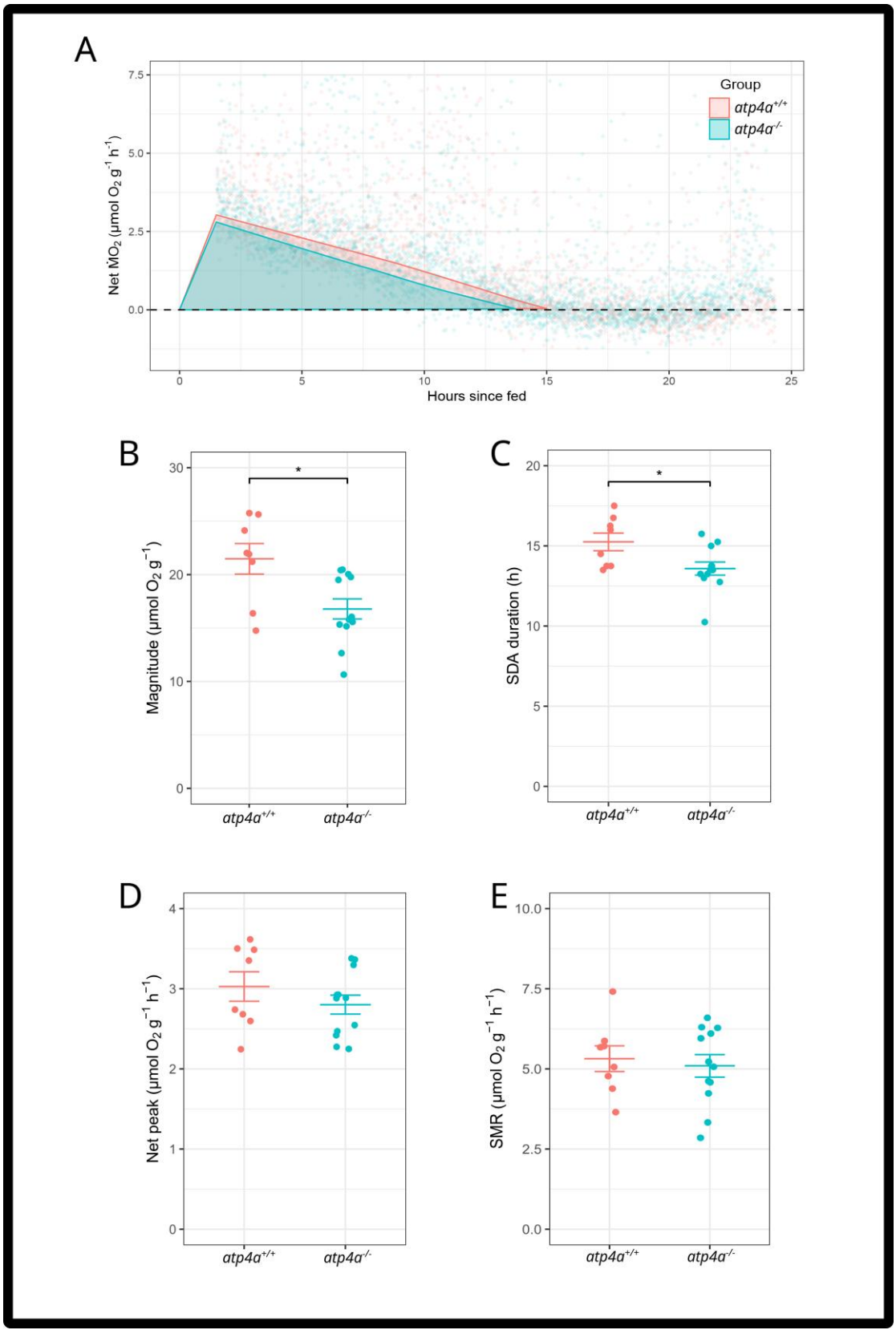

Fig. 3. Change in oxygen consumption rate over time in *A. mexicanus* voluntarily fed a 5% BM meal of bloodworms (n = 8 *atp4a*$^{+/+}$ and n=12 *atp4a*$^{-/-}$). In **A**, points show the recorded $\dot{M}O_2$ values for all individuals of both groups, while polygons show the average SDA area for each group (i.e. individual SDA values for each time point were averaged for this representation). To ease visualization of the SDA polygons, the y-axis in plot **A** was truncated at 7.5 $\mu molO_2\ g^{-1}\ h^{-1}$; hiding 276 individual $\dot{M}O_2$values (corresponding to 4.8% of the full dataset). **B-E** illustrate the (**B**) magnitude, (**C**) duration, (**D**) net peak and (**E**) SMR in both genotypes. Significant differences ($p < 0.05$) between genotypes are identified by asterisks.

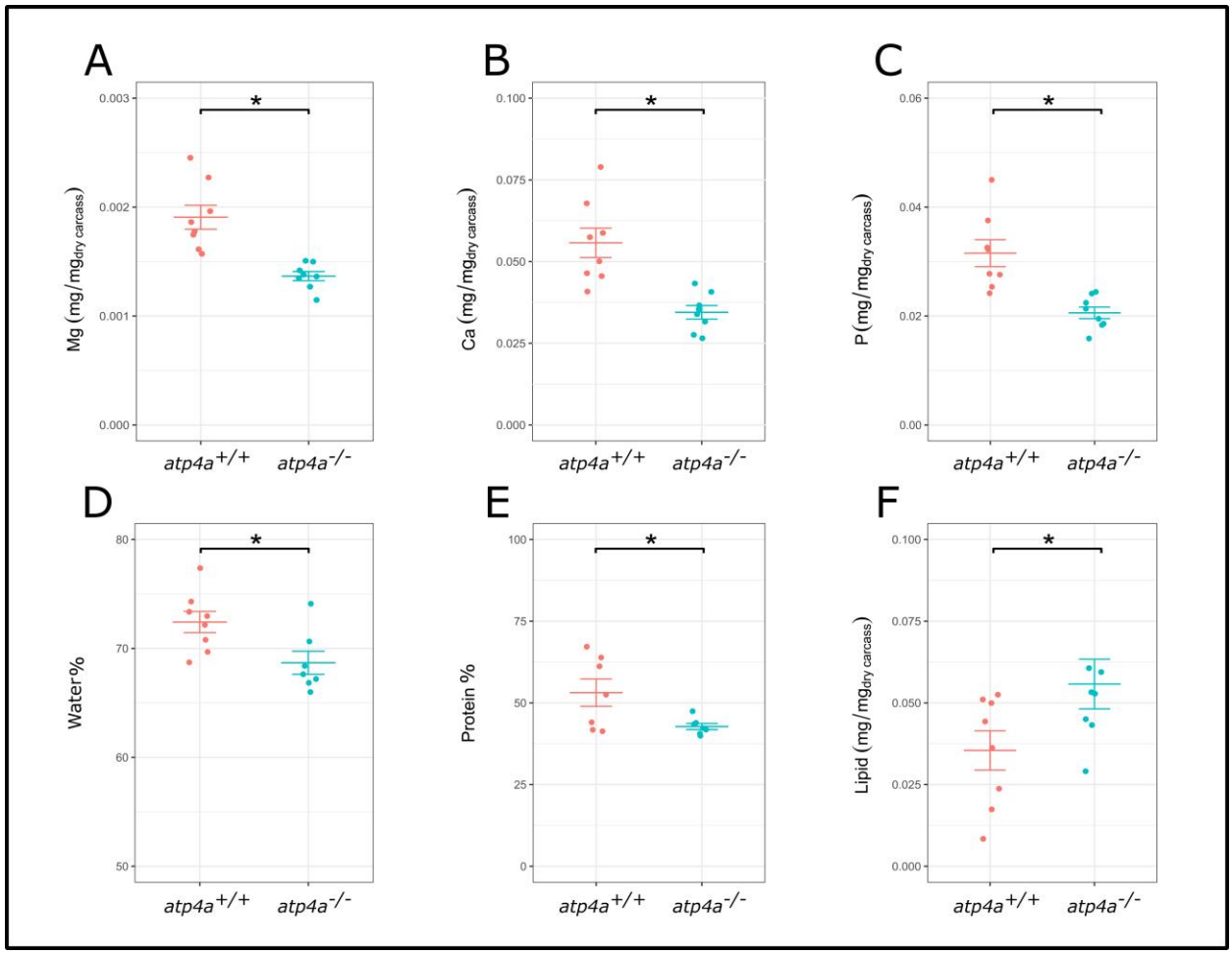

Fig. 4. Carcass analyses show significantly lower levels of (**A**) Mg^{+2}, (**B**) Ca^{+2} and (**C**) P^{+}, in *atp4a*$^{-/-}$ fish. The percentage of water (**D**) and protein (**E**) in the carcass of *atp4a*$^{-/-}$ is significantly reduced, while lipid content is increased, (**F**). Asterisks indicate a significant difference between genotypes, p-value < 0.05.

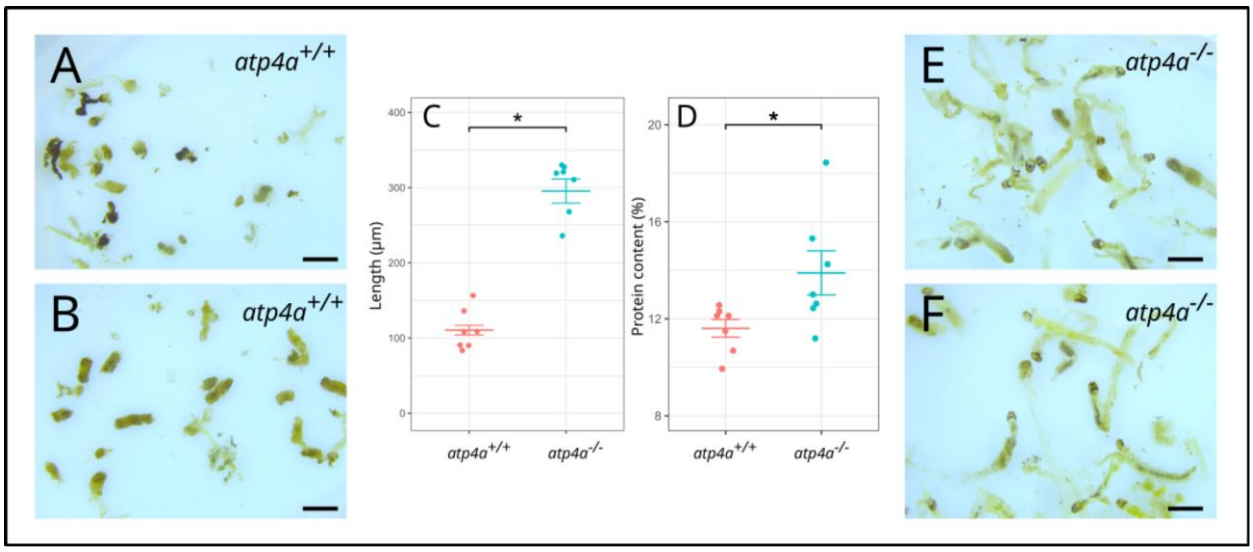

Fig. 5. Changes in digestibility assessed through fecal analysis of animals fed bloodworms.

Visual comparison between *atp4a*$^{+/+}$ (A,B) and *atp4a*$^{-/-}$ (E,F) faeces shows apparent more intact matter in *atp4a*$^{-/-}$ faeces. These differences are corroborated by a statistically shorter length of the faeces and significantly higher protein content in fecal matter from *atp4a*$^{-/-}$ fish (C, D). Scale bars 100 µm, n=8, p-value < 0.05.

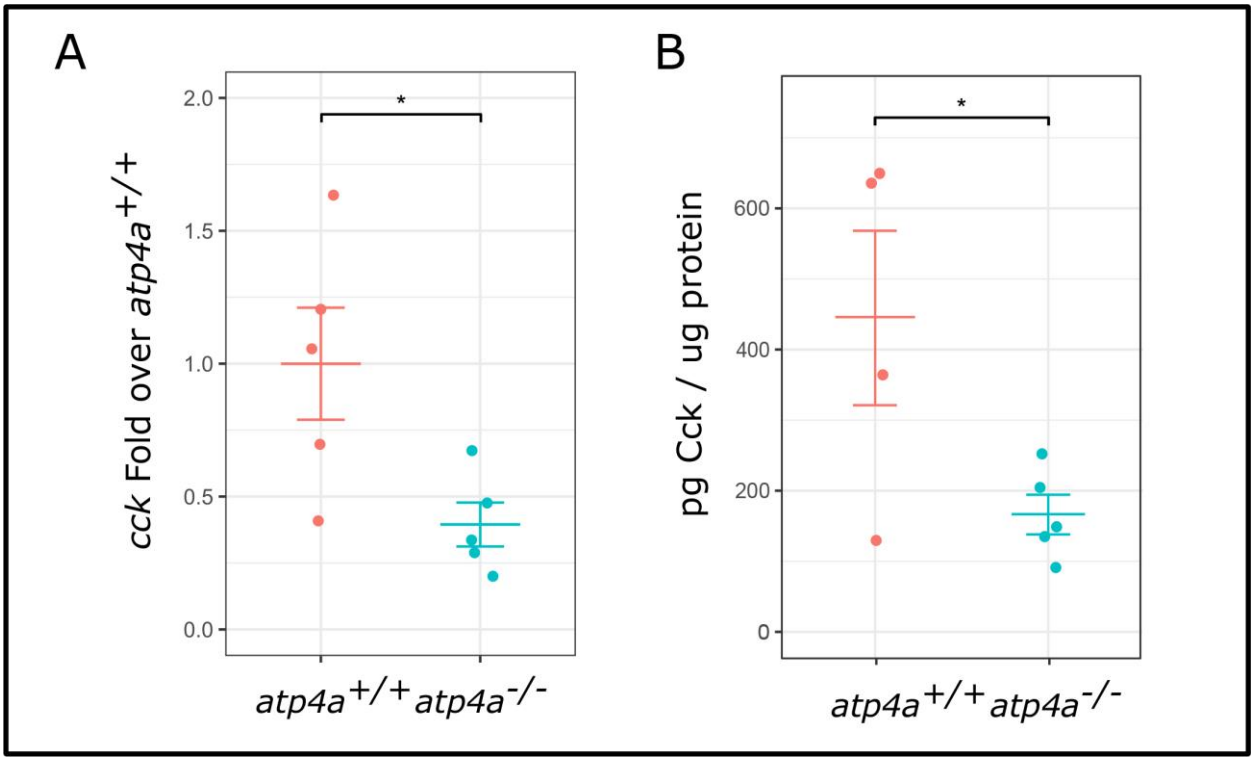

Fig. 6. Changes in anterior intestine *cck* transcript (**A**) and Cck enzyme (**B**) levels at 3h post-feed in *atp4a*$^{+/+}$ and *atp4a*$^{-/-}$*A. mexicanus*. Asterisks indicate significant differences between genotypes, p-value < 0.05.

Table 1. Primers used in the study and qPCR efficiency values (E) and accession number.

Gene	Forward Primer	Reverse Primer	E	Accession number
lepa	CAACGAGATGAGCTGCCGAT	CAGGCCTTCGATGGGCTTAT	103.2%	XM_049483678.1
mc4r	GGACAGTAATTGACTGCTGCTT	ACGTGGCACCATGTTGTACT	106.1%	XM_007232098.4
insra	CGAGCCAAAAGCTCCCAATG	GCTTACAGCCATTGTCCGTG	92.8%	XM_007236326.4
npy	ACGAGGCAGAGGTATGGGAA	ATCACCACATCAACGGGTCG	89.7	XM_049476010.1
pyy	GAAAACCCAGGAGACGATGC	CCCTCTGGAGTGGACCTTTT	108.2	XM_022671994.2
ghra	GCATTCGACAACTTTGGGGA	ATCCCCACCACACCAAACA	98.9	XM_049485692.1
ghrb	CAAGTGCTCTTCAACGTGGA	AGCGACACTCAGTAAAGTCCA	98.1	XM_022675925.2
cckb	AAGGTGGAGATGTAGGTGCA	GCTCTCCTTGAACTTGCAGG	95.3	XM_022676228.2

Supplementay Materials and Methods

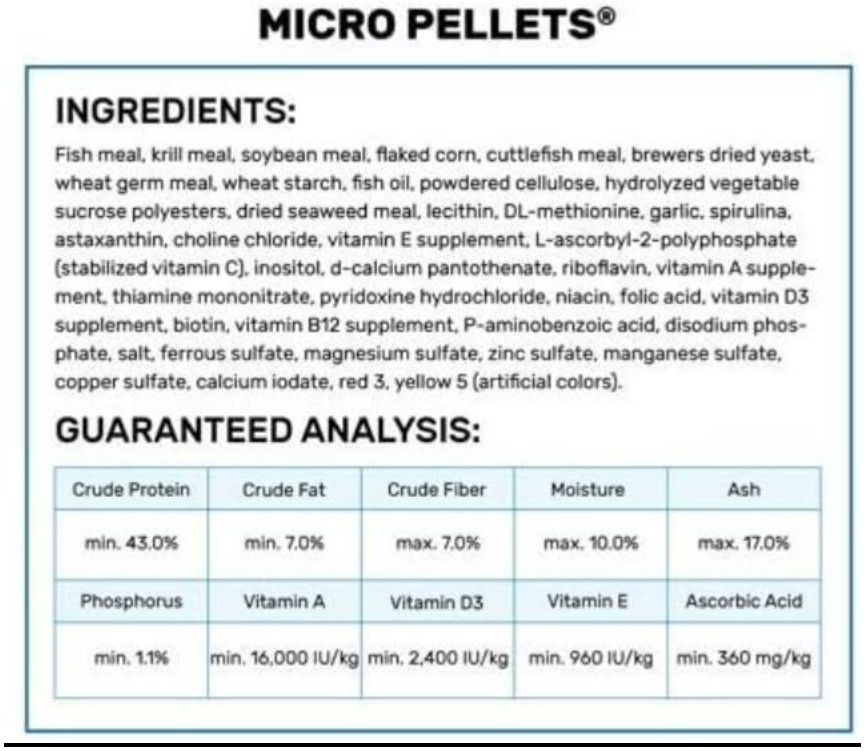

MICRO PELLETS®

INGREDIENTS:

Fish meal, krill meal, soybean meal, flaked corn, cuttlefish meal, brewers dried yeast, wheat germ meal, wheat starch, fish oil, powdered cellulose, hydrolyzed vegetable sucrose polyesters, dried seaweed meal, lecithin, DL-methionine, garlic, spirulina, astaxanthin, choline chloride, vitamin E supplement, L-ascorbyl-2-polyphosphate (stabilized vitamin C), inositol, d-calcium pantothenate, riboflavin, vitamin A supplement, thiamine mononitrate, pyridoxine hydrochloride, niacin, folic acid, vitamin D3 supplement, biotin, vitamin B12 supplement, P-aminobenzoic acid, disodium phosphate, salt, ferrous sulfate, magnesium sulfate, zinc sulfate, manganese sulfate, copper sulfate, calcium iodate, red 3, yellow 5 (artificial colors).

GUARANTEED ANALYSIS:

Crude Protein	Crude Fat	Crude Fiber	Moisture	Ash
min. 43.0%	min. 7.0%	max. 7.0%	max. 10.0%	max. 17.0%
Phosphorus	**Vitamin A**	**Vitamin D3**	**Vitamin E**	**Ascorbic Acid**
min. 1.1%	min. 16,000 IU/kg	min. 2,400 IU/kg	min. 960 IU/kg	min. 360 mg/kg

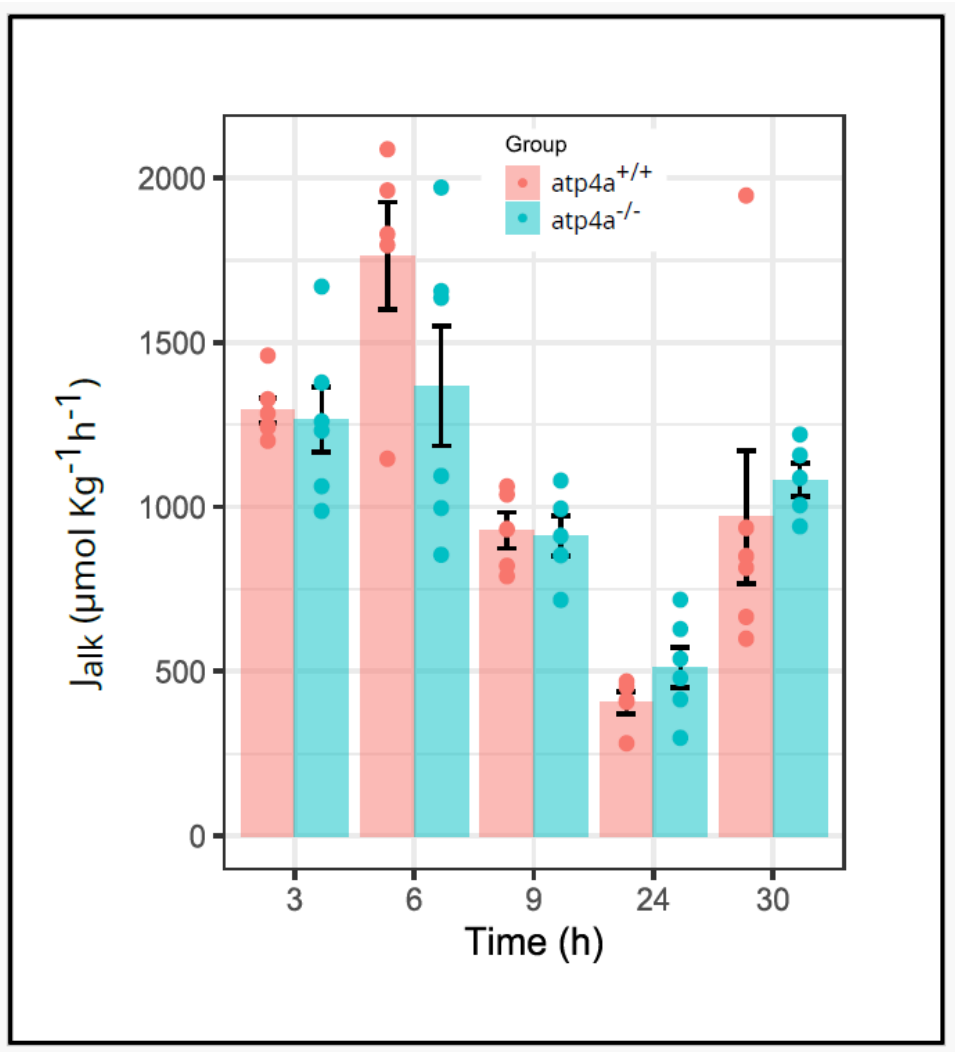

Fig. S1. Water titratable alkalinity of *A. mexicanus atp4a*$^{+/+}$ and *atp4a*$^{-/-}$ fed a 5% BM ration of bloodworms (n = 8 per group). Data are presented as mean ± SEM.

Brain transcriptional analysis

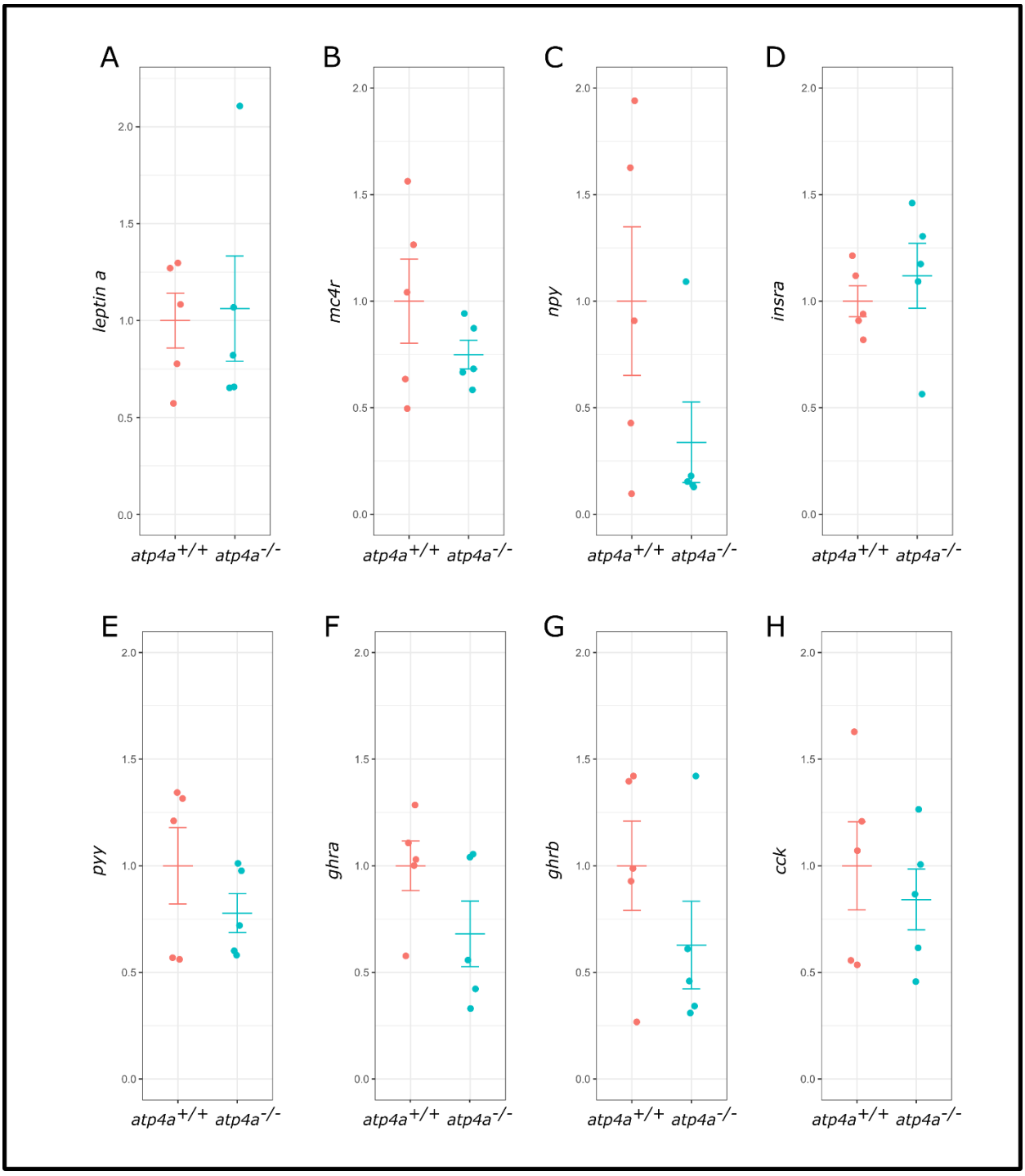

Fig. S2. Analysis of transcriptional changes of selected genes related to satiation and growth in brain tissue. The brain mRNA levels for *leptin a* (**A**), *mc4r* (**B**), *npy* (**C**), *insra* (**D**), *pyy* (**E**), *ghra* (**F**), *ghrb* (**G**) and *cck* (**H**) remained unaltered between groups at 3h post-feed. Gene expression presented as fold over *atp4a*$^{+/+}$fish. t-test $p < 0.05$.

Carcass analysis

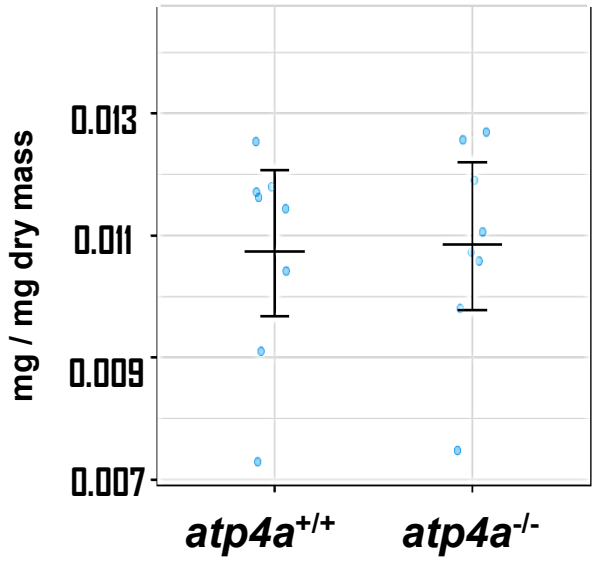

Fig. S3. Carcass sodium content (mg Na /mg dry mass). Groups compared by t-test. No significant differences.

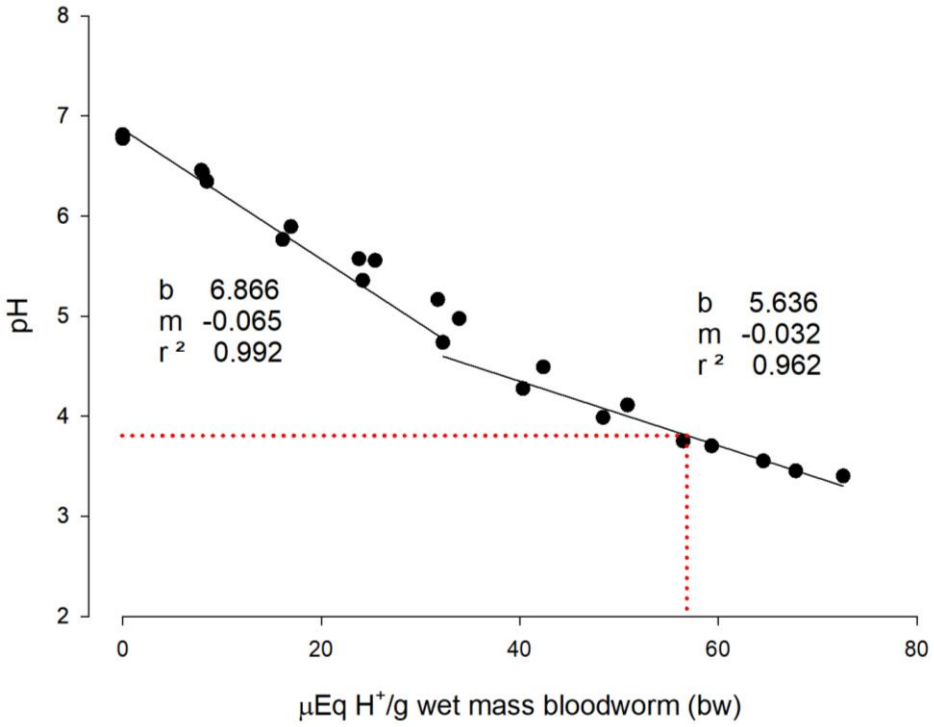

pH Range 6.8-5.0
Gastric acid secreted = [(pHbw-pHst) - 6.866] / -0.065
pH Range < 5.0
Gastric acid secreted = [(pHbw-pHst) - 5.636] / -0.032

Fig. S4. Titration curve showing the net acid secretion required for the bloodworm meal to reach pH 3.8 (red dotted line, value based on Ferreira et al., 2024b).

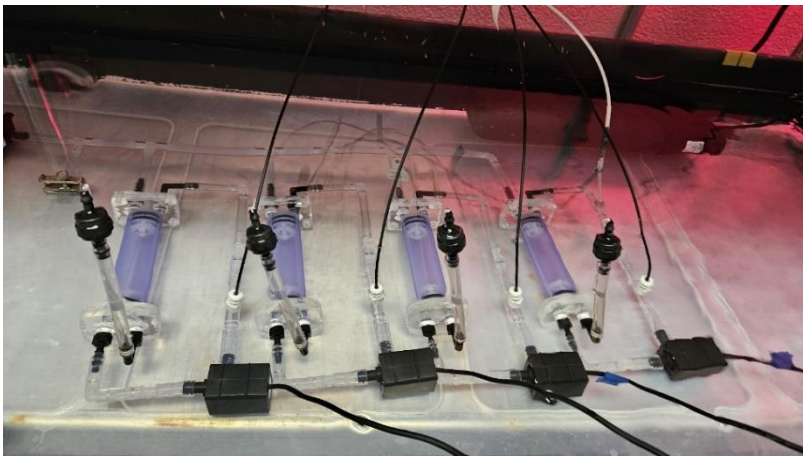

Fig. S1. Respirometry system used in the present study.

Appetite

Table S1. Comparison of appetite [worms consumed (mg/K)], Fulton's condition factor (K), and gastric evacuation [gastric content (wet mass)/ ration (wet mass)] between *atp4a*$^{+/+}$ and *atp4a*$^{-/-}$ fish. Welsh t-test.

	worms consumed (mg/K)	**K**	**Stomach Contents**
atp4a$^{+/+}$	4.38 ± 0.21	2.09 ± 0.06	0.18 ± 0.02
atp4a$^{-/-}$	4.66 ± 0.19	1.97 ± 0.07	0.18 ± 0.03
t_{df}	$t_{8.5}$= 1.01	$t_{12.7}$= 1.65	$T_{13.9}$= 0.02
p-value	0.34	0.12	0.98

Supplementary methods

Lipid extraction and determination

Briefly, 10-20 mg of ground carcass was weighed into 2 ml tubes containing 1.8 mL of chloroform and methanol mixture (2:1) and incubated overnight at room temperature with agitation in a fume-hood. Following incubation, 0.2mL of 0.9M NaCl was added and thoroughly mixed by vortexing and incubated for 6h at room temperature followed by a centrifugation at 2.5k x g for 5 min. After centrifugation, the chloroform phase was transferred into a new pre-weighed (using an ultramicrobalance SE2, Sartorius) 1.5mL tube. The tubes were left open in a fumehood at room temperature for 72h until all the chloroform had evaporated. Following this, the tubes were reweighed using the ultramicrobalance and the total lipid was calculated and expressed as a percentage of the dry mass.

Respirometry

The setup consisted of a water bath (approx. 43L) equipped with a portable UV filter and aeration, where four custom-built respirometers were placed. The respirometers were made of clear PVC pipe (inner diameter = 2cm; length = 6 cm) with a total volume of 24 mL including the recirculation tubing. Water temperature during experiments ranged between 21.8 and 23.8°C ($\bar{x}$ = 22.3°C), using an aquarium heater connected to a temperature control system (ITC-306T, Inkbird Tech CL, China). Each respirometer was rinsed with 70% alcohol and left to dry between every run to minimize background oxygen consumption. The respirometers were equipped with O2 probes (OXFLOW-HS; PyroScience GmbH, Aachen, Germany) connected to a PyroScience Firesting O2 sensor (FSO2-C4; PyroScience GmbH). Water temperature was monitored with a temperature probe (TDIP15; PyroScience GmbH) placed within the recirculation loop of one of the chambers. In-chamber oxygen concentration and temperature were measured every second. The flow of water within the chamber was maintained at a level that allowed for accurate O2 measurements but without causing turbulence or disturbance of the fish inside (using 5V pumps, model AD20P-0510A, Shenzhen Giant Electric Tech Inc). One flush pump (same model) was used to flush all four respirometers. The custom-built flush controller was set to perform cycles of 3 min measurement and 2 min flush. The first 60 s of the measurement data were discarded (wait phase). Background oxygen consumption was measured both before adding the animals and after their removal (x-y cycles), to correct for any microbial consumption of O2 that could otherwise have confounded the measurements.

$\dot{M}_{O_2}$ and SDA calculations

The $\dot{M}_{O_2}$ for each cycle was determined using the R package pyroresp (Flávio, 2025), in R v4.4.1 (R Core Team, 2024). The recorded O2 values (hPa) were converted to µmol O2 L-1 h-1 using the respirometry R package (Birk, 2024). Changes in background respiration were linearly modeled over time to correct recorded oxygen readings. The corrected O2 readings were used to determine

Journal of Experimental Biology • Supplementary information

the slope and R2 of the lines of best fit for each cycle. Cycles with an R2 > 0.9 were considered valid for the determination of $\dot{M}_{O_2}$. SMR was determined by calculating the quantile 0.2 for the pre-feeding $\dot{M}_{O_2}$ values of each animal (Chabot et al., 2016a). SDA was determined using a modified version of the functions provided by Chabot et al. (2016b). Specifically, the function rqss() from the quantreg R package (Koenker et al., 2018) was used to fit an additive quantile regression model to the postprandial $\dot{M}_{O_2}$ data for each animal, with lambda = 24, and tau = 0.2. Trials with fasted animals showed that it takes approximately 1 h for the fish to reduce its O2 consumption to resting levels after being placed in the chamber. As such, data collected during the first 1.5 h post-feeding were not used for SDA determination. Fitted values were predicted for every 15 min interval after the discarded period. The fitted values were used to determine the duration, peak in net $\dot{M}_{O_2}$, and magnitude (the latter using the function trap.rule() from the R package Hmisc; Harrell Jr et al., 2019).

References

Chabot, D., Koenker, R., & Farrell, A. (2016a). The measurement of specific dynamic action in fishes. Journal of Fish Biology, 88 (1), 152–172.

Chabot, D., Steffensen, F., & Farrell, A. (2016b). The determination of standard metabolic rate in fishes. Journal of Fish Biology, 88 (1), 81−121.

Flávio, H. (2025). pyroresp: Analyse respirometry data captured by firesting loggers. https://github.com/hugomflavio/pyroresp

Harrell Jr, F. E., Harrell, J., & Maintainer, F. E. (2019). Package hmisc. CRAN2018, 2019, 235−236.

Koenker, R., Portnoy, S., Ng, P. T., Zeileis, A., Grosjean, P., & Ripley, B. D. (2018). Package ‘quantreg.